8.A.1 Nuclear Physics B38 (1972) 477-528. North-Holland Publishing Company

# RIGOROUS SPIN TESTS FROM USUAL STRONG DECAYS

M. G. DONCEL
*Departamento de Fisica Teórica,*
*Universidad Autónoma de Barcelona,*
*Sardañola, Barcelona, Spain*

L. MICHEL
*Institut des Hautes Etudes Scientifiques,*
91, *Bures-sur-Yvette, France*

P. MINNAERT
*Laboratoire de Physique Théorique,*
*Université de Bordeaux I,*
33, *Talence, France*

Received 22 July 1971

Abstract: Applying our geometrical formalism, we make a general study of angular momentum and parity conservation in the most frequent two body strong decays, in order to propose new tests for the determination of the spin of the decaying particle.

## 1. INTRODUCTION

Determination of spin value can be partially based on any general physical principle *, established law ** or proposed model ***. However it ultimately relies upon the conservation of angular momentum. In this paper we present some new considerations on rigorous spin tests based only on angular momentum and parity conservation.

The efficiency of spin tests depends on many factors. It may happen that one can unambiguously determine a spin from one particular experiment, or from a small fraction of the known experimental data. If this is not the

* The principle of detailed balancing assumes time reversal invariance. The two reactions $\pi^+ d^+ \rightleftharpoons p^+ p^+$ helped to determine the $\pi^+$ meson spin: ref. [3]. Isoparity conservation is useful to eliminate spin values of a new non-strange meson resonance M of isospin $t$: ex. $M \rightarrow 2\pi$, $j + t$ is even: ref. [4].

** Brehmsstrahlung and pair production cross sections increase rapidly with spin $j$: ref. [5] established for the cosmic ray $\mu$-particle $j \leq \frac{1}{2}$.

*** As an example of study of spin determination based on the quark model, see ref. [6].

case, one wants to know how to use the full data, without loss of information, for the spin determination.

In a previous work (ref. [1]) we implicitly solved this problem. Indeed we explain there how to construct the domain $\hat{\mathcal{D}}_j$ of polarization density matrices which can be observed in a given kind of experiments, when one assumes a value $j$ for the spin; and we explicitly construct domains $\hat{\mathcal{D}}_j$ for $j \leq \frac{5}{2}$. Angular momentum and parity conservation can only exclude the conjectured values of $j$, for which the representative point of the experimental data is outside $\hat{\mathcal{D}}_j$.

Here we apply our general method explicitly to the problem of spin determination from angular distribution measurements. Without any assumption on the $j$ value, the result of the experiment is described by a point in a space $\mathcal{Y}$ in which the domains $\hat{\mathcal{D}}_j$ can also be represented for all $j$ values (and even for the limit $j \to \infty$). As we will see, in the concrete examples we study, there are regions of $\mathcal{Y}$ common to all $\hat{\mathcal{D}}_j$ and other regions contained only in one, or very few, $\hat{\mathcal{D}}_j$. If the experimental point falls in one of the former regions, the experiment has no potential usefulness for spin determination. If it falls in a region of the latter case, one has a strong incentive to increase the experimental accuracy!

Consider the three most frequent strong decay modes:

(a) the two parity conserving meson decays of the type:

$$j^{\eta} \to 0^- + 0^- \,, \quad \text{necessarily with natural parity} \quad \eta = (-1)^j \,, \tag{1}$$

$$j^{\eta} \to 1^- + 0^- \,, \quad \text{when the parity is natural,} \quad \eta = (-1)^j \,, \tag{1'}$$

(b) the parity conserving baryon decay of the type:

$$j \to \tfrac{1}{2} + 0^- \text{ with any parity} \,. \tag{2}$$

The angular distribution of their decay products depends only on the spin and polarization of the decaying particle and *not* on the dynamics of the decay. It contains only $L$-even spherical harmonics up to $L_0 \leq 2j$.

In sect. 2 we present a summary of our geometrical study of the polarization domain and of the method to translate the data of an angular distribution into a point of the polarization space. In sect. 3 we give a complete study of the decays (1), (1') and (2) when $L_0 = 2$. Sect. 4 contains a partial but practical study of the same decays when $L_0$ is larger.

## 2. GENERAL FORMALISM

This section contains an abstract of some parts of refs. [1, 2]. It presents a geometrical description of the polarization of a particle, and of the relation with the angular distribution of its two-body decay products.

### 2.1. *Polarization domain*

2.1.1. We consider here the polarization states of one particle of mass $m > 0$ and spin $j$ for a given value $p$ of its energy-momentum ($p^2 = m^2$). Each polarization state is described by a density matrix $\rho$, which represents a

Hermitean, trace one, non negative linear operator acting on the $(2j+1)$-dimensional Hilbert space $\mathcal{H}_{2j+1}$:

$$\rho^* = \rho\ , \qquad \mathrm{tr}\,\rho = 1\ , \qquad \rho \geqslant 0\ . \tag{3}$$

We call $\mathcal{E}_{N+1}$ the real vector space of all $(2j+1)$ by $(2j+1)$ Hermitean matrices, and $\mathcal{E}_N$ the hyperplane of trace one Hermitean matrices. Their dimension are respectively $N+1$ and $N$ with $N = (2j+1)^2 - 1$. The set of $\rho$ which satisfy eqs. (3) is a subdomain $\mathcal{D}_j$ of $\mathcal{E}_N$:

$$\mathcal{D}_j \subset \mathcal{E}_N \subset \mathcal{E}_{N+1}\ . \tag{4}$$

It is a *convex domain*, called the polarization domain.

2.1.2. The vector space $\mathcal{E}_{N+1}$ is a Euclidean space with the natural scalar product:

$$(\rho_1,\ \rho_2) = \mathrm{tr}\,\rho_1\,\rho_2\ . \tag{5}$$

The *metric* (5) on $\mathcal{E}_{N+1}$ induces a Euclidean metric on $\mathcal{E}_N$. We choose the unpolarized state, whose density matrix is

$$\rho_0 = \frac{1}{2j+1}\,\mathbb{1}\ , \tag{6}$$

as origin for the vector space $\mathcal{E}_N$. States such that

$$\rho^2 = \rho \tag{7}$$

are the pure states. The degree of polarization $d_\rho$ of any state $\rho$ is proportional to its distance to the unpolarized state $\rho_0$. As we normalize $d_\rho$ to 1 for pure states, it is given by:

$$0 \leqslant d_\rho = \left[\frac{2j+1}{2j}\,(\rho-\rho_0,\ \rho-\rho_0)\right]^{\frac{1}{2}} \leqslant 1\ . \tag{8}$$

Therefore it is convenient to introduce in $\mathcal{E}_N$ the metric induced by (5) with the normalization (8):

$$d(\rho_1,\ \rho_2) = \left[\frac{2j+1}{2j}\,(\rho_1-\rho_2,\ \rho_1-\rho_2)\right]^{\frac{1}{2}} = \left[\frac{2j+1}{2j}\,\mathrm{tr}\,(\rho_1-\rho_2)^2\right]^{\frac{1}{2}}\ . \tag{9}$$

2.1.3. Let us study the *rank* of matrices $\rho$, i.e., the number of their non zero eigenvalues. The density matrix of a pure state is a rank one projector whose eigenvector (defined up to a factor) is the state vector. The domain $\mathcal{D}_j$ is the convex hull of the pure states. The matrices $\rho$ of the interior of $\mathcal{D}_j$ have rank $n = 2j+1$. On the boundary, $\partial\,\mathcal{D}_j$, the matrices have a rank $k$ strictly smaller than $n$. The dimension of the manifold $\partial_k\,\mathcal{D}_j$ of density matrices of rank $k$ is:

$$\dim\,\partial_k\,\mathcal{D}_j = 2nk - k^2 - 1\ . \tag{10}$$

2.1.4. The little group of $p$, i.e. the subgroup of the orthochronous Lorentz group which leaves invariant the energy-momentum $p$, is isomorphic to $0(3)$, the three dimensional orthogonal group. So we call its elements "rotations" and "reflections" because they are conjugated of genuine rotations and reflections by the "boost" which transforms the particle

from rest to the velocity $\boldsymbol{p}/E$ with $p = (E, \boldsymbol{p})$. This group acts on $\mathcal{H}_{2j+1}$ by the irreducible linear representation $D^{(j,\eta)}$ ($j$ spin, $\eta$ parity) and, on $\mathcal{E}_N$, by the reducible linear representation (up to an equivalence)

$$\oplus_{L=1}^{2j} D^{(L,+)} . \tag{11}$$

In the corresponding decomposition of $\mathcal{E}_N$,

$$\mathcal{E}_N = \oplus_{L=1}^{2j} \mathcal{E}^{(L)} , \tag{12}$$

the $(2L+1)$-dimensional space $\mathcal{E}^{(L)}$ carries the components of the $2^L$th-multipole $\rho^{(L)}$. Indeed the direct decomposition (12) corresponds, for each density operator $\rho$, to the multipole expansion:

$$\rho = \rho_0 + \sum_{L=1}^{2j} \rho^{(L)} . \tag{13}$$

2.1.5. The *effective* polarization domain, $\hat{\mathcal{D}}_j$, of the density matrices of a spin $j$ particle that can be actually produced in a given kind of reactions, may be smaller than $\mathcal{D}_j$. Let us consider three examples of such production conditions:

(i) The production reaction conserves parity, the beam and target are unpolarized, and there are only three linearly independent observed energy-momenta; e.g. quasi two-body reactions such that

$$\pi^+ p \to K^{*+} \Sigma^+ , \tag{14}$$

$$\pi^- p \to \pi^- N^{*-} , \tag{15}$$

where $K^*$ and $N^*$ are resonant states of unknown spin. The space-time hyperplane which contains the observed energy-momenta is a symmetry plane for the reaction. We note $B$ the "reflection" through this plane ‡. This reflection acts on $\mathcal{H}_{2j+1}$ by $D^{(j,\eta)}(B)$ and on $\mathcal{E}_N$ by a symmetry through a $k$-dimensional plane $\mathcal{E}^{(B)}$. Therefore the domain $\hat{\mathcal{D}}_j$ of "*B-symmetric*" density matrices is the intersection

$$\mathcal{D}_j^{(B)} = \mathcal{D}_j \cap \mathcal{E}^{(B)} . \tag{16}$$

The dimension of $\mathcal{D}_j^{(B)}$ is also $k$:

$$k = 2j(j+1) \qquad \text{for } j \text{ integer} , \tag{17}$$

$$k = 2j(j+1) - \tfrac{1}{2} \qquad \text{for } j \text{ half-integer} . \tag{17'}$$

Note that $\mathcal{D}_j^{(B)}$ is a convex domain, since it is the intersection (16) of two convex domains. (For more details see refs. [1, 2], IA3).

(ii) The production reaction is *collinear*, e.g. forward or backward production of particles in a two-body reaction with unpolarized target and

‡ The vocabulary "$B$-symmetry" is in reference to Å. Bohr [7].

beam. Then $\mathcal{D}_j$ is the intersection $\mathcal{D}_j^{(C)}$ of $\mathcal{D}_j$ with a $k'$-dimensional plane $\mathcal{C}^{(C)}$. The domain $\mathcal{D}_j^{(C)}$ is convex and has dimension $k' = 2j+1$.

(iii) The production reaction imposes a restriction on the *rank* of the final particle density matrix. Indeed the rank of the product of matrices is smaller than or equal to the smallest rank of the matrices of the product. Hence the polarization density matrix of the final state,

$$\rho_f = T\rho_i T^* , \tag{18}$$

cannot have a larger rank than that of $\rho_i$, the polarization density matrix of the initial state. For instance in reaction (15) the density matrix of the $N^*$ has

$$\text{rank } \rho(N^*) \leq 2 . \tag{19}$$

Note also that the rank of the sum of matrices cannot be larger than the sum of their rank. So in reaction (14), if the polarization of the $\Sigma^+$ is not observed one must complete eq. (18) by a summation over the two polarization states of the $\Sigma^+$; then the rank condition for the density matrix of the $K^*$ becomes

$$\text{rank } \rho(K^*) \leq 4 , \tag{20}$$

which is a constraint if the $K^*$ has spin >1. (For more details see refs. [1, 2]).

2.1.6. Often, the density matrix cannot be completely measured. Therefore the *observed* polarization domain $\hat{\mathcal{D}}_j$ is the projection of $\mathcal{D}_j$ on the $k$-plane of measurable parameters. For instance, the angular distribution of the decay products in a parity conserving two-body decay contains only even-$L$ spherical harmonics. In other words, this decay is not sensitive to the odd-$L$ multipoles $\rho^{(L)}$ of $\rho$. What is observed is then the projection of $\rho$ on the subspace

$$\mathcal{C}^{(E)} = \oplus_{L \text{ even}} \mathcal{C}^{(L)} \subset \mathcal{C}_N . \tag{21}$$

2.1.7. Let us study some *symmetry* properties of a convex domain $\mathcal{D}$ which will allow us to relate the production and observation conditions we have considered. Let $P_1$, $P_2 \ldots$ be projectors of $\mathcal{C}_N$, orthogonal with respect to the scalar product (9). Each projection $P_i\mathcal{D}$ of the convex domain $\mathcal{D}$ is convex and it contains the intersection by $P_i\mathcal{C}_N$:

$$P_i\mathcal{D} \supset (\mathcal{D} \cap P_i \mathcal{C}_N) . \tag{22}$$

When projection and intersection coïncide, we say that $P_i \mathcal{C}_N$ is an equatorial plane of $\mathcal{D}$. A symmetry plane of $\mathcal{D}$ is an equatorial plane, but the converse is not always true (think of the equatorial plane of an egg!). For instance, the diagonal matrices form an equatorial $2j$-plane of $\mathcal{D}_j$ which is not a symmetry plane. When $P_iP_j = P_jP_i$ the planes $P_i \mathcal{C}_N$ and $P_j \mathcal{C}_N$ are perpendicular‡. The intersection of perpendicular equatorial planes is an

‡ We should have said that the two planes are perpendicular or that one is included in the other, but for short we call them perpendicular. As a special case, the planes $P_i \mathcal{C}_N$ and $P_j \mathcal{C}_N$ are said to be orthogonal if $P_iP_j = P_jP_i = 0$.

equatorial plane. Note that the intersection of two perpendicular symmetry planes is not in general a symmetry plane. However if $\mathcal{E}_i$ is any plane perpendicular to the symmetry plane $\mathcal{E}_S$, then $\mathcal{E}_S$ and $\mathcal{E}_S \cap \mathcal{E}_i$ are symmetry planes of the intersection $\mathcal{D} \cap \mathcal{E}_i$ and of the projection $P_i\mathcal{D}$.

The planes $\mathcal{E}^{(E)}$ and $\mathcal{E}^{(B)}$ that we have introduced are examples of perpendicular symmetry planes of the polarization domain $\mathcal{D}_j$. So their intersection $\mathcal{E}^{(E,B)}$ is a symmetry plane for both subdomains $\mathcal{D}_j^{(E)}$ and $\mathcal{D}_j^{(B)}$. Furthermore the symmetries through $\mathcal{E}^{(E)}$ and $\mathcal{E}^{(B)}$ transform any matrix $\rho$ into a matrix $\rho'$ of same rank. Therefore the rank of e.g. the projection $P_E\rho$ is

$$\text{rank } P_E\rho = \text{rank } \tfrac{1}{2}(\rho + \rho') \leqslant 2 \text{ rank } \rho \,. \tag{23}$$

For instance in reactions (14) and (15), if one observes only the even polarization of the $K^*$ and $N^*$ (through their parity conserving decays) eqs. (20) and (19) impose that the observed density matrices have a rank

$$\text{rank } \rho^{(E)}(K^*) \leqslant 8 \,, \tag{24a}$$

$$\text{rank } \rho^{(E)}(N^*) \leqslant 4 \,. \tag{24b}$$

These are constraints for spin values $j(K^*) > 3$, $j(N^*) > \frac{3}{2}$.

2.1.8. We prove in appendix A.1 another useful geometrical property of $\mathcal{D}_j$, namely its invariance under the *polar transformation* with respect to the sphere $S$ centered at $\rho_0$ and of radius

$$R = \sqrt{\frac{-1}{2j}} \,.$$

As a consequence, for any plane $\mathcal{E}_i$ containing $\rho_0$, the intersection $\mathcal{E}_i \cap \mathcal{D}_j$ and the projection $P_i\mathcal{D}_j$ are polar transforms of each other with respect to the sphere $S \cap \mathcal{E}_i$. Therefore when $\mathcal{E}_i$ is an equatorial plane $\mathcal{E}_i \cap \mathcal{D}_j = P_i\mathcal{D}_j$ is self transformed.

2.2. *Angular distribution domain for two-body decays*

2.2.1. For a two body decay, we denote by $\mathcal{I}(\theta, \varphi)$ the normalized angular distribution of one of the decay products. It is a real, normalized (i.e. its integral is unity), non negative function defined on the unit sphere $\Omega$ of the three-dimensional space orthogonal to $p$, the energy-momentum of the decaying particle ‡:

$$\overline{\mathcal{I}(\theta, \varphi)} = \mathcal{I}(\theta, \varphi) \,, \tag{25a}$$

$$\int_\Omega \mathcal{I}\, d\Omega \equiv \int_{-1}^{+1} \int_0^{2\pi} \mathcal{I}(\theta, \varphi)\, d\cos\theta\, d\varphi = 1 \,, \tag{25b}$$

‡ The coordinates $\theta$, $\varphi$ of $\Omega$ give the space directions of the considered decay products for any rest frame of the decaying particle. Of course, these coordinates can be defined in a covariant way from the energy momenta of the involved particles. (cf. ref. [8].)

$$\mathcal{I}(\theta, \varphi) \geqslant 0 . \tag{25c}$$

We call $\mathcal{Y}'$ the Hilbert space of square integrable functions on $\Omega$ with the scalar product

$$\langle \mathcal{I}_1, \mathcal{I}_2 \rangle = \int \bar{\mathcal{I}}_1 \mathcal{I}_2 \, d\Omega . \tag{26}$$

We are interested in the "angular distribution space", i.e. in the subspace $\mathcal{Y}$ of functions which satisfy eqs. (25a) and (25b). The functions of $\mathcal{Y}$ which, in addition, satisfy eq. (25c) form the "angular distribution domain", $\Delta$. It is a convex domain containing the isotropic angular distribution

$$\mathcal{I}_0 = \frac{1}{4\pi} . \tag{27}$$

Any measurement of a two-body decay angular distribution can be represented by a point

$$y \in \Delta \subset \mathcal{Y} \subset \mathcal{Y}' .$$

The group of "rotations" and "reflections" (little group of $p$ isomorphic to 0(3)) acts on $\Omega$, and therefore on $\mathcal{Y}'$.

It leaves $\mathcal{I}_0$ invariant; its action on $\mathcal{Y}$ is the real linear representation

$$D = \oplus_{L=1}^{\infty} D^{(L,+)} , \tag{28}$$

which yields the *multipole decomposition* of the space $\mathcal{Y}$

$$\mathcal{Y} = \oplus_{L=1}^{\infty} \mathcal{Y}^{(L)} , \tag{29}$$

and the multipole expansion of an angular distribution

$$\mathcal{I} = \mathcal{I}_0 + \sum_{L=1}^{\infty} \mathcal{I}^{(L)} . \tag{30}$$

2.2.2. The *parallel* to the previous subsection is obvious. We can introduce symmetry planes and equatorial planes of $\Delta$, such as $\mathcal{Y}^{(E)}$ and $\mathcal{Y}^{(B)}$, for which the intersection, $\Delta^{(E)}$ and $\Delta^{(B)}$, coincides with the projection. We will prove in appendix A. 2 that the domain $\Delta$ is also invariant under the polar transformation with respect to the sphere centered at the point $\mathcal{I}_0$ and of imaginary radius

$$R = \sqrt{\frac{-1}{4\pi}} .$$

Thus, also, for any $k$-plane of $\mathcal{Y}$ containing $\mathcal{I}_0$, projection and intersection are polar transforms of each other.

2.2.3. Consider the two-body decay of a spin $j$ particle in a polarization state $\rho \in \mathcal{D}_j$. The decay angular distribution $\mathcal{I}$ is a linear function of $\rho$. Geometrically, the decay mode (i) of a spin $j$ particle is therefore represented by a *linear mapping*

Table 1
Decay coefficients $\lambda_i(L, j)$ for the modes $(i) = (1), (1'), (2)$.

(a) Decay coefficients for mode (1) $[j \to 0 + 0]$

$$\sqrt{4\pi}\lambda_1(L,j) = (-1)^j [2j(2j+1)]^{\frac{1}{2}} \begin{pmatrix} j & j & L \\ 0 & 0 & 0 \end{pmatrix}$$

$$= \begin{cases} 0, & \text{for odd } L \\ (-1)^{\frac{1}{2}L} \binom{L}{\frac{1}{2}L} (j+\frac{1}{2}L)^{[L]} [(2j+L+1)^{[L]} (2j-1)^{[L-1]}]^{-\frac{1}{2}}, & \\ & \text{for even } L . \end{cases}$$

To interpret, cf. (d) below; e.g.:

$$\sqrt{4\pi}\lambda_1(2,j) = -j\,[2(j+1)/(2j+3)(2j-1)]^{\frac{1}{2}}$$

$$\sqrt{4\pi}\lambda_1(4,j) = 3j[(j+2)(j+1)(j-1)/2(2j+5)(2j+3)(2j-1)(2j-3)]^{\frac{1}{2}}$$

(b) Decay coefficients for mode (1') $[j^\eta \to 1^- + 0^-,\ \eta = (-1)^j]$

$$\sqrt{4\pi}\lambda_{1'}(L,j) = (-1)^{j-1} [2j(2j+1)^3]^{\frac{1}{2}} \begin{Bmatrix} j & j & L \\ j & j & 1 \end{Bmatrix} \begin{pmatrix} j & j & L \\ 0 & 0 & 0 \end{pmatrix}$$

$$= \begin{cases} 0, & \text{for odd } L \\ (-1)^{\frac{1}{2}L} \binom{L}{\frac{1}{2}L} (j+\frac{1}{2}L)^{[L]} [1 - L(L+1)/2j(j+1)] [(2j+L+1)^{[L]} (2j-1)^{[L-1]}]^{-\frac{1}{2}} & \\ & \text{for even } L . \end{cases}$$

To interpret, cf. (d) below; e.g.:

$$\sqrt{4\pi}\lambda_{1'}(2,j) = -2\,[j(j+1)-3]\,[(2j+3)(2j+2)(2j-1)]^{-\frac{1}{2}}$$

$$\sqrt{4\pi}\lambda_{1'}(4,j) = 3\,[j(j+1)-10]\,[(j+2)(j-1)/2(2j+5)(2j+3)(j+1)(2j-1)(2j-3)]^{\frac{1}{2}}$$

(c) Decay coefficients for mode (2) $[j \to \frac{1}{2} + 0]$

$$\sqrt{4\pi}\lambda_2(L,j) = (-1)^{j-\frac{1}{2}} [2j(2j+1)]^{\frac{1}{2}} \begin{pmatrix} L & j & j \\ 0 & \frac{1}{2} & -\frac{1}{2} \end{pmatrix} \frac{1+(-1)^L}{2}$$

$$= \begin{cases} 0, & \text{for odd } L \\ (-1)^{\frac{1}{2}L} \binom{L}{\frac{1}{2}L} (j+\frac{1}{2}(L+1))^{[\frac{1}{2}L]} (j-\frac{1}{2})^{[\frac{1}{2}L]} [(2j+L+1)^{[L]} (2j-1)^{[L-1]}]^{-\frac{1}{2}} & \\ & \text{for even } L . \end{cases}$$

To interpret, cf. (d) below; e.g.:

$$\sqrt{4\pi}\lambda_2(2,j) = -\tfrac{1}{2}\,[(2j+3)(2j-1)/(2j+2)]^{\frac{1}{2}}$$

$$\sqrt{4\pi}\lambda_2(4,j) = \tfrac{3}{8}\,[(2j+5)(2j+3)(2j-1)(2j-3)/(2j+4)(2j+2)(2j-2)]^{\frac{1}{2}}$$

(d) Shorthands: $\binom{a}{b} = \dfrac{a!}{b!\,(a-b)!}$; $a^{[b]} = \dfrac{a!}{(a-b)!}$

$$\mathcal{E}_N \xrightarrow{\lambda_i(j)} \mathcal{Y} . \tag{31}$$

So the angular distribution of the decay mode (i) of a particle in the polarization state $\rho$ is represented by the point

$$y = \lambda_i(j)[\rho] . \tag{32}$$

Poincaré invariance requires this mapping to be equivariant‡ for the "rotations" of the little group of $p$. This implies that $\lambda_i(j)$ maps each multipole subspace $\mathcal{E}_N^{(L)}$ into the corresponding $\mathcal{Y}^{(L)}$

$$\mathcal{E}_N^{(L)} \xrightarrow{\lambda_i(L,\, j)} \mathcal{Y}^{(L)} ,$$

and that these $\lambda_i(L, j)$ mappings reduce to multiplication by a scalar. We denote these scalars also by $\lambda_i(L, j)$ and call them *decay coefficients*.

As we announced in the introduction, these coefficients do not depend on the dynamics for the decay modes (i) = (1), (1'), (2); they are functions of $j$ and $L$ only. These functions are given in table 1. On these examples, one can verify that for two body decays, angular momentum conservation implies

$$\lambda_i(L, j) = 0 \quad \text{for} \quad L > 2j , \tag{34}$$

and parity conservation implies (cf. ref. [2])

$$\lambda_i(L, j) = 0 \quad \text{for} \quad L \text{ odd} . \tag{35}$$

2.2.4. In this paper, we are interested in spin tests from the angular distribution in decay modes (i) = (1), (1'), (2). The procedure will be to represent this experimental angular distribution, $\mathcal{D}$, by a point $y \in \mathcal{Y}$. In any case, it must belong to $\Delta$. In addition, for each spin value $j$, we can consider in $\mathcal{Y}$ the domain

$$\lambda_i(j)[\hat{\mathcal{D}}_j] = \lambda_i(j)[\hat{\mathcal{D}}_j^{(E)}] \tag{36}$$

that, in short, we will denote by $\lambda_i\, \mathcal{D}_j$. The values of $j$ for which the corresponding domain $\lambda_i\, \mathcal{D}_j$ does not contain the experimental point $y$, are excluded by the experiment.

2.3. *Multipole expansions*

2.3.1. It is customary to use for a basis in the complexified of the space $\mathcal{N}+1$, the real, non Hermitean matrices $T(j)_M^{(L)}$ whose elements are:

$$(T(j)_M^{(L)})_{m'}^{m} = \langle j\, m' LM \,|\, j\, m\rangle = \sqrt{2j+1} \begin{pmatrix} m & L & j \\ j & M & m' \end{pmatrix} . \tag{37}$$

‡ This word, commonly used in the mathematic literature, means that the image by $\lambda$ of a rotated point of $\mathcal{E}_N$ is the rotated of the image point by the same rotation in $\mathcal{Y}$.

They transform under a rotation $R$ according to the law:

$$D^{(j)}(R)\, T(j)^{(L)}_{M}\, D^{(j)}(R)^{-1} = T(j)^{(L)}_{M'}\, D^{(L)}(R)^{M'}_{M} \,. \tag{38}$$

So any Hermitean matrix $\rho$ acting on $\mathcal{H}_{2j+1}$ can be expanded in this basis:

$$\rho = \sum_{L=0}^{2j} \sum_{M=-L}^{+L} \sqrt{\frac{2L+1}{2j+1}}\, \overline{t^{(L)}_{M}}\, (T(j)^{(L)}_{M}) \,; \tag{39}$$

and one shows that the *multipole parameters* $t^{(L)}_{M}$ satisfy:

$$(\mathrm{tr}\,\rho = 1 \Rightarrow)\ t^{(0)}_{0} = 1 \,, \tag{40}$$

$$(\rho^{*} = \rho \Rightarrow)\ \overline{t^{(L)}_{M}} = (-1)^{M} t^{(L)}_{-M} \,. \tag{41}$$

The degree of polarization $d_\rho$ defined in (8) is

$$d_\rho = \Big( \sum_{L=1}^{2j} \sum_{M=-L}^{+L} \frac{2L+1}{2j} \, |t^{(L)}_{M}|^{2} \Big)^{\frac{1}{2}} \,. \tag{42}$$

2.3.2. We prefer (cf. ref. [1, 2]) to introduce a real orthonormal basis of $\mathcal{E}_N$, made with Hermitean matrices

$$Q(j)^{(L)}_{0} = \sqrt{\frac{2L+1}{2j}}\, T^{(L)}_{0} \,, \tag{43a}$$

$$(0 < M \leq L) \begin{cases} Q(j)^{(L)}_{M} = (-1)^{M} \sqrt{\dfrac{2L+1}{j}}\, \tfrac{1}{2} \left( T(j)^{(L)}_{M} + T(j)^{(L)^{*}}_{M} \right) & \text{(43b)} \\ Q(j)^{(L)}_{-M} = (-1)^{M} \sqrt{\dfrac{2L+1}{j}}\, \dfrac{1}{2i} \left( T(j)^{(L)}_{M} - T(j)^{(L)^{*}}_{M} \right) , & \text{(43c)} \end{cases}$$

such that

$$(Q(j)^{(L)}_{M},\, Q(j)^{(L')}_{M'}) = \frac{2j+1}{2j}\, \delta_{LL'}\, \delta_{MM'} \,. \tag{44}$$

We denote by $r^{(L)}_{M}$ the coordinates of $\rho$ in this orthonormal basis:

$$\rho = \rho_{0} + \frac{2j}{2j+1} \sum_{L=1}^{2j} \sum_{M=-L}^{+L} Q(j)^{(L)}_{M}\, r^{(L)}_{M} \,. \tag{45}$$

The degree of polarization is, as function of these *normalized* multipoles parameters $r^{(L)}_{M}$,

$$d_\rho = \Big( \sum_{L=1}^{2j} \sum_{M=-L}^{+L} (r^{(L)}_{M})^{2} \Big)^{\frac{1}{2}} \,. \tag{46}$$

Table 2
Multipole parameters.

(a) Multipole parameters of the polarization space $\mathcal{E}_N$

$$r_M^{(L)} = \mathrm{tr}\rho Q_M^{(L)} = \begin{cases} (-1)^M \sqrt{(2L+1)/j}\ \mathrm{Re}\, t_M^{(L)}, & \text{for } M > 0; \\ \sqrt{(2L+1)/2j}\ t_0^{(L)}, & \text{for } M = 0; \\ (-1)^M \sqrt{(2L+1)/j}\ \mathrm{Im}\, t_{-M}^{(L)}, & \text{for } M < 0. \end{cases}$$

(b) Multipole parameters of the angular distribution space $\mathcal{Y}$

$$y_M^{(L)} = \langle Y_M^{(L)} \rangle = \int \mathcal{I}(\theta, \varphi)\, Y_M^{(L)}(\theta, \varphi)\, \mathrm{d}\cos\theta\, \mathrm{d}\varphi$$

(c) Relation between the multipole parameters in (a) and (b)

$$y_M^{(L)} = \sqrt{\frac{2L+1}{2j}}\lambda_i(L, j)\, t_M^{(L)}$$

$$\lambda_i(L,j) r_M^{(L)}(j) = \begin{cases} (-1)^M \sqrt{2}\ \mathrm{Re}\, y_M^{(L)}, & \text{for } M > 0 \\ y_0^{(L)}, & \text{for } M = 0 \\ (-1)^M \sqrt{2}\ \mathrm{Im}\, y_{-M}^{(L)}, & \text{for } M < 0 \end{cases}$$

(For concrete values of $\lambda_i(L, j)$, see table 1.)

For $j = \frac{1}{2}$, the $Q_M^{(1)}$ are the Pauli matrices and the three $r_M^{(1)}$ are the components of the usual polarization vector. The explicit relations between the $r_M^{(L)}$ and the $t_M^{(L)}$ are given in table 2a.

2.3.3. It is customary to choose as an orthonormal basis of the Hilbert space $\mathcal{Y}'$ the spherical harmonics $Y_M^{(L)}(\theta, \varphi)$,

$$\left\langle Y_M^{(L)}, Y_{M'}^{(L')} \right\rangle = \int_{-1}^{+1} \int_0^{2\pi} \overline{Y_M^{(L)}(\theta, \varphi)}\, Y_{M'}^{(L')}(\theta, \varphi)\, \mathrm{d}\cos\theta\, \mathrm{d}\varphi = \delta_{LL'}\delta_{MM'}. \quad (47)$$

We denote (cf. table 2b) by $y_M^{(L)}$ the expectation value $\langle Y_M^{(L)} \rangle$ of the spherical harmonics for the angular distribution $\mathcal{I}$. They are the components of the representing point $y \in \mathcal{Y}$; the expansion of $\mathcal{I}$ in spherical harmonics reads

$$\mathcal{I}(\theta, \varphi) = \frac{1}{4\pi} + \sum_{L=1}^{\infty} \sum_{M=-L}^{+L} \overline{y_M^{(L)}}\, Y_M^{(L)}(\theta, \varphi). \quad (48)$$

The reality of $\mathcal{I}$ implies

$$\overline{y_M^{(L)}} = (-1)^M y_{-M}^{(L)}. \quad (49)$$

For a particle of spin $j$ and density matrix $\rho$ with the explicit form given in eq. (39), the angular distribution, $y = \lambda_i(j)[\rho]$, for the two-body decay mode (i), reads

$$\mathcal{I}(\theta, \varphi) = \frac{1}{4\pi} + \sum_{L=1}^{2j} \sqrt{\frac{2L+1}{2j}} \lambda_i(L, j) \sum_{M=-L}^{+L} \overline{t_M^{(L)}}\, Y_M^{(L)}(\theta, \varphi) \,. \tag{50}$$

The coefficient in front of $\lambda_i(L, j)$ is the square root of that which enter in the expression for $d_\rho^2$, cf. eq. (41). It disappears when one uses the normalized multipole parameters $r_M^{(L)}$ (cf. table 2c).

## 3. QUADRUPOLE ANGULAR DISTRIBUTION.

From the preceding study we are now able to discuss the efficiency of spin tests from observed quadrupole angular distribution. We will apply this discussion to the decay modes (1), (1'), (2).

### 3.1. *Geometry of the quadrupole domains*

3.1.1. We need to study the following domains: the quadrupole intersection and projection of the $j$-dependent polarization domain,

$$\mathcal{D}_j^{(2)} = \mathcal{D}_j \cap \mathcal{E}^{(2)} \,, \qquad \widetilde{\mathcal{D}}_j^{(2)} = P^{(2)} \mathcal{D}_j \,, \tag{51}$$

and of the angular distribution domain from two body decays,

$$\Delta^{(2)} = \Delta \cap \mathcal{Y}^{(2)} \,, \qquad \widetilde{\Delta}^{(2)} = \mathcal{P}^{(2)} \Delta \,, \tag{52}$$

where $P^{(2)}$ and $\mathcal{P}^{(2)}$ are the orthogonal projectors on the quadrupole subspaces of respectively $\mathcal{E}_N$ and $\mathcal{Y}$. Since $\mathcal{D}_j$, $\mathcal{E}^{(2)}$, $\Delta$, $\mathcal{Y}^{(2)}$ are invariant by 0(3), the little group of $p$, the domains (51) and (52) are *invariant* too.

3.1.2. The group 0(3) acts on $\mathcal{E}^{(2)}$ and $\mathcal{Y}^{(2)}$ by its irreducible linear representation $D^{(2,+)}$. But since the "reflection" through the origin acts trivially, we consider only the action of S0(3), cf. e.g. eq. (38). This action decomposes $\mathcal{E}^{(2)}$ and $\mathcal{Y}^{(2)}$ in orbits. The dimension of the orbit space is

$$\nu_2 = \dim \mathcal{E}^{(2)} - \dim \mathrm{S0(3)} = 5 - 3 = 2 \,, \tag{53}$$

i.e. two algebraically *independent invariants* are necessary to characterize each orbit. As we saw in subsect. 2.2, the dilation $\lambda(2, j)$ maps $\mathcal{E}^{(2)}$ onto $\mathcal{Y}^{(2)}$ for each value of $j$ and each understood decay mode (i). Therefore the same invariants (up to a factor) can be used for the orbit spaces of $\mathcal{E}^{(2)}$ and $\mathcal{Y}^{(2)}$. The unitary representation $D^{(2)}$ is equivalent to a real, therefore orthogonal, representation; it preserves the length of vectors. We choose as first invariant:

$$\alpha = \sum_{M=-2}^{+2} (\lambda r_M^{(2)})^2 = \sum_{M=-2}^{+2} |y_M^{(2)}|^2 \,. \tag{54a}$$

We establish in appendix A.4 that another algebraically independent invariant is

$$\beta = \lambda^3 \Big\{ r_0^{(2)} \Big[ r_0^{(2)2} - 3 \left( r_2^{(2)2} + r_{-2}^{(2)2} \right) + \tfrac{3}{2} \left( r_1^{(2)2} + r_{-1}^{(2)2} \right) \Big] + \tfrac{3}{2}\sqrt{3} \left( r_1^{(2)2} - r_{-1}^{(2)2} \right) r_2^{(2)} + 3\sqrt{3}\, r_1^{(2)} r_{-1}^{(2)} r_{-2}^{(2)} \Big\}$$

$$= y_0^{(2)} \Big[ |y_0^{(2)}|^2 - 3 \left( |y_2^{(2)}|^2 + |y_{-2}^{(2)}|^2 \right) + \tfrac{3}{2} \left( |y_1^{(2)}|^2 + |y_{-1}^{(2)}|^2 \right) \Big] + 3\sqrt{6}\, \mathrm{Re} \left( y_1^{(2)2} y_{-2}^{(2)} \right) . \tag{54b}$$

We have given the invariants in the space $\mathcal{Y}^{(2)}$; to obtain the invariants in the space $\mathcal{C}^{(2)}$, put $\lambda = 1$ everywhere and consider only the first equality in eqs. (54). In both spaces these two invariants satisfy the necessary and sufficient conditions (cf. appendix A.4)

$$\alpha \geqslant 0 , \qquad -\alpha^{\frac{3}{2}} \leqslant \beta \leqslant \alpha^{\frac{3}{2}} . \tag{55}$$

In the following, we will prefer another set of two algebraically independent invariants, $\lambda\xi$, $\lambda\eta$, because they are homogeneous to the coordinates $\lambda r_M^{(2)}$ or $y_M^{(2)}$. The algebraic relations between the old and the new invariants are:

$$\alpha = \lambda^2(\xi^2 + \eta^2) , \qquad \beta = \lambda^3 \eta(\eta^2 - 3\xi^2) . \tag{56}$$

To inverse these relations ‡, define $\omega$ by:

$$-\tfrac{1}{2}\pi \leqslant 3\omega \leqslant \tfrac{1}{2}\pi , \qquad \sin 3\omega = -\beta\alpha^{-\frac{3}{2}} . \tag{57a}$$

Then $\lambda\xi$, $\lambda\eta$ are defined by

$$\lambda\xi = \sqrt{\alpha}\cos\omega , \qquad \lambda\eta = \sqrt{\alpha}\sin\omega . \tag{57b}$$

We also prove in appendix A.4 that all points of $\mathcal{C}^{(2)}$ or $\mathcal{Y}^{(2)}$ which have the same values of $\alpha$, $\beta$, or of $\lambda\xi$, $\lambda\eta$, are on the same orbit of SO(3), i.e. they can be transformed into each other by a "rotation".

The sector $-\frac{1}{6}\pi \leqslant \omega \leqslant \frac{1}{6}\pi$ of the two-plane $\lambda\xi$, $\lambda\eta$ is therefore the orbit space of $\lambda\mathcal{C}^{(2)} = \mathcal{Y}^{(2)}$ for the action of SO(3) ‡‡.

We will find it more convenient to use below the full two-plane $\{\lambda\xi , \lambda\eta\}$. Then, in general, each orbit is represented by six points, which are transforms of each other by a group $\mathcal{S}_3$ (isomorphic to the permutation group of three objects), generated by the symmetry through the axes

$$\omega = \tfrac{1}{6}(2n+1) \qquad \xi = 0 , \quad \sqrt{3}\,\eta \pm \xi = 0 . \tag{58}$$

This group $\mathcal{S}_3$ contains also the rotations by $\frac{2}{3}\pi$ around the origin. The orbits with $|\omega| = \frac{1}{6}\pi$ cut the two-plane $\{\lambda\xi, \lambda\eta\}$ in three points only, one on

‡ One cannot give $\lambda\xi$, $\lambda\eta$ as real expressions in $\alpha, \beta$ or $\lambda r_M^{(2)} \sim y_M^{(2)}$ with the ordinary algebraic symbols including $\sqrt{}$.

‡‡ The situation is similar to that of the Dalitz plot for three identical particles. The five dimensional phase space is invariant by 0(3), the little group of the total energy momentum, and by the group of permutations of the particles. The orbit space is a $\frac{1}{3}\pi$ sector of the Dalitz plot.

each symmetry axis. We shall call the two-plane $\{\lambda\xi, \lambda\eta\}$, "two-plane of meridian sections". We shall explain why below.

3.1.3. Let us choose a quantization tetrad and consider the two-plane of $\mathcal{Y}^{(2)} = \lambda\, \mathcal{E}^{(2)}$ spanned by the coordinates $\lambda r_2^{(2)}$ and $\lambda r_0^{(2)}$. Two such two-planes, corresponding to two choices of quantization tetrads, are transformed into each other by the "rotation" which transforms the quantization tetrads into each other. We then verify that each orbit $\xi, \eta$ cuts each two-plane of this family. Indeed, eqs. (54) to (57) show that in such a two-plane

$$\xi = r_2^{(2)} , \qquad \eta = r_0^{(2)} . \tag{59}$$

Therefore we can identify the abstract two-plane $\{\lambda\xi, \lambda\eta\}$ with the two-plane $\{\lambda r_2^{(2)}, \lambda r_0^{(2)}\}$ corresponding to an arbitrary quantization tetrad.

Any SO(3) invariant domain $\lambda\, \mathcal{D}_{\text{inv}}$ (e.g. $\lambda\, \mathcal{D}_j^{(2)}$, $\lambda\, \widetilde{\mathcal{D}}_j^{(2)}$, $\Delta^{(2)}$, $\widetilde{\Delta}^{(2)}$) is a union of SO(3) orbits, and, according to eq. (59), it is generated by a $\frac{1}{3}\pi$ "meridian sector" of the "*meridian section*",

$$\{\lambda r_2^{(2)}, \lambda r_0^{(2)}\} \cap \lambda\, \mathcal{D}_{\text{inv}} . \tag{60}$$

That is the reason why we call "two-plane of meridian section" any plane $\{\lambda r_2^{(2)}, \lambda r_0^{(2)}\}$ and also the abstract plane $\{\lambda\xi, \lambda\eta\}$.

For any $\lambda\, \mathcal{D}_{\text{inv}}$, the two-plane of meridian section $\{\lambda r_2^{(2)}, \lambda r_0^{(2)}\}$ is not in general a symmetry plane, but it is always an equatorial plane. Indeed the SO(3) invariants $\alpha$, $\beta$ given in eqs. (54) are invariant for the symmetries

$$\lambda r_M^{(2)} \to \epsilon_M \lambda r_M^{(2)} \quad \text{with} \quad (\epsilon_M)^2 = 1 , \tag{61}$$

such that

$$\epsilon_0 = \epsilon_2 = 1 , \qquad \epsilon_{-2}\, \epsilon_1\, \epsilon_{-1} = 1 . \tag{61'}$$

Hence for any quantization tetrad, the three three-planes $\{\lambda r_2^{(2)}, \lambda r_0^{(2)}, \lambda r_{-2}^{(2)}\}$, $\{\lambda r_2^{(2)}, \lambda r_0^{(2)}, \lambda r_1^{(2)}\}$, $\{\lambda r_2^{(2)}, \lambda r_0^{(2)}, \lambda r_{-1}^{(2)}\}$ are symmetry planes of each orbit, and therefore of any $\mathcal{D}_{\text{inv}}$. That is not the case for the two-plane $\{\lambda r_2^{(2)}, \lambda r_0^{(2)}\}$; but, as it is the intersection of perpendicular symmetry planes, it is an equatorial plane for any convex, invariant domain, $\mathcal{D}_{\text{inv}}$ (cf. subsect. 2.1.7).

Consider the quadrupole component of the polarization of a spin-$j$ particle. We have just shown that one can always choose the quantization tetrad such that the only non vanishing $r_M^{(2)}$ are $r_2^{(2)}$ and $r_0^{(2)}$. Outside the exceptional cases $\beta^2 = \alpha^3$, the right-handed tetrad is uniquely defined up to the labelling and the sign of its axes. Hence, a quadrupole polarization is completely characterized by this tetrad and the two invariants $\xi$, $\eta$; the $\frac{1}{3}\pi$ sector of the point $\xi$, $\eta$ depends on the labelling of the tetrad axes.

3.1.4. The *B-symmetric* domain $\lambda\mathcal{D}_j^{(B)}$ has dimension $k < N$ (cf. eq. (17)) and it is not invariant by 0(3) but only by the subgroup 0(2) of "rotations" around the normal to the reaction plane and the "reflections" through this plane. In particular the domains $\lambda\mathcal{D}_j^{(B,2)} = \lambda\mathcal{D}_j^{(B)} \cap \mathcal{E}^{(2)}$ and $\lambda\tilde{\mathcal{D}}_j^{(B,2)} = \lambda P^{(2)}\,\mathcal{D}_j^{(B)}$ are three-dimensional and have only one axis of revolution. Their meridian section by a two-plane containing this axis is identical to the meridian section of the S0(3)-invariant full quadrupole domains $\lambda\mathcal{D}_j^{(2)}$ and $\lambda\tilde{\mathcal{D}}_j^{(2)}$. Indeed it is easy to verify (see eqs. (63) and (64) below) that the two-plane $\{\lambda r_2^{(2)},\ \lambda r_0^{(2)}\}$ is also a two-plane of meridian section for the 0(2)-invariant $\lambda\mathcal{D}_j^{(B,2)}$ and $\lambda\tilde{\mathcal{D}}_j^{(B,2)}$ in either transversity or helicity quantization.

The coordinates of the $B$-symmetric polarization states depend on the choice of quantization axis (cf. ref. [1]). For quadrupole $B$-symmetric polarization the non-vanishing coordinates of $\mathcal{E}^{(B,2)}$ and of $\mathcal{Y}^{(B,2)} = \lambda\,\mathcal{E}^{(B,2)}$ and the invariants $\lambda\xi$, $\lambda\eta$ are:

(a) in any transversity quantization:

$$r_0^{(2)},\ r_2^{(2)},\ r_{-2}^{(2)}\ ;\qquad y_0^{(2)},\ y_2^{(2)}\ \text{(complex)}\ ;$$

$$\lambda\eta = \lambda r_0^{(2)} = y_0^{(2)}\ ; \tag{62a}$$

$$\lambda\xi = \lambda\left(r_2^{(2)2} + r_{-2}^{(2)2}\right)^{\frac{1}{2}} = \sqrt{2}\,|y_2^{(2)}| = \sqrt{2}\,|y_{-2}^{(2)}|\ , \tag{62b}$$

(b) in any helicity quantization:

$$r_0^{(2)},\ r_1^{(2)},\ r_2^{(2)}\ ;\quad y_0^{(2)},\ y_1^{(2)} = -y_{-1}^{(2)}\ \text{(real)},\ y_2^{(2)} = y_{-2}^{(2)}\ \text{(real)}\ ;$$

$$\lambda\eta = -\tfrac{1}{2}\lambda(r_0^{(2)} + \sqrt{3}r_2^{(2)}) = -\tfrac{1}{2}(y_0^{(2)} + \sqrt{6}y_2^{(2)})\ , \tag{63a}$$

$$\lambda\xi = \tfrac{1}{2}\lambda\left[(r_2^{(2)} - \sqrt{3}r_0^{(2)})^2 + 4r_1^{(2)2}\right]^{\frac{1}{2}} = \frac{1}{\sqrt{2}}\left[(y_2^{(2)} - \sqrt{\tfrac{3}{2}}y_0^{(2)})^2 + 4y_1^{(2)2}\right]^{\frac{1}{2}}\ . \tag{63b}$$

Those equations are independent of the spin $j$. In the simplest case of spin-one or $\frac{3}{2}$, there still are experimental papers which prefer to give, instead of the $r_M^{(L)}$, the value of the matrix elements of the density matrix $\rho$. For arbitrary $B$-symmetric state, in any helicity quantization (such as $s$-helicity, $t$-helicity = Jackson axes, etc.) the invariants $\xi$, $\eta$ are, as function of the $\rho_{mm'}$ for spin-one,

$$\eta = \tfrac{1}{2} - \tfrac{3}{2}(\rho_{11} + \rho_{1-1})\ , \tag{64a}$$

$$\xi = \frac{\sqrt{3}}{2}\left[(\rho_{00} - \rho_{11} + \rho_{1-1})^2 + 8\rho_{10}{}^2\right]^{\frac{1}{2}} \tag{64b}$$

of the $\rho_{2m,2m'}$ for spin-$\frac{3}{2}$,

$$\eta = -\frac{1}{\sqrt{3}}(\rho_{33} - \rho_{11}) - 2\rho_{3-1}\,, \tag{65a}$$

$$\xi = \left[\left(\frac{2}{\sqrt{3}}\rho_{3-1} - \rho_{33} + \rho_{11}\right)^2 + \tfrac{16}{3}\ \rho_{31}{}^2\right]^{\frac{1}{2}}. \tag{65b}$$

For the particular case of $B$-symmetric, even polarization, spin-one density matrices $\rho$, in $t$-helicity quantization Donohue and Högaasen [9] have already given as invariants the $\rho$ eigenvalues, $\frac{1}{3}(1-2\eta)$ and $\frac{1}{3}(1+\eta \pm \xi\sqrt{3})$, and noticed the existence of the intrinsic tetrad that we introduced before (at the end of subsect. 3.1.3). They also give the angle of the rotation, around the normal to the reaction plane, which transforms their quantization tetrad into the intrinsic tetrad.

3.1.5. We need to study the *rank* of the polarization matrices $\rho$ which are pure quadrupole: $\rho \in \mathcal{D}_j^{(2)}$. The points of the interior of $\mathcal{D}_j^{(2)}$ represent matrices $\rho$ with maximal rank, i.e. rank $\rho = 2j+1$. The rank is strictly smaller for the points of the boundary (cf. subsect. 2.1)

$$\partial\mathcal{D}_j^{(2)} = \partial\mathcal{D}_j \cap \mathcal{E}^{(2)}\,. \tag{66}$$

From a detailed study of $\partial\mathcal{D}_j^{(2)}$, using refs. [1, 2] 1A6, one shows that all points of $\partial\mathcal{D}_j^{(2)}$ have same rank except, when $j$ is integer, for three "exceptional" points which are on the symmetry axes (58). One of them has for coordinates:

$$\xi = 0\,, \qquad \eta = -\left[\sqrt{10j(j+1)}\begin{pmatrix} j & j & 2 \\ j & -j & 0 \end{pmatrix}\right]^{-1} = -\frac{1}{j}\sqrt{\frac{(2j+3)(2j+1)}{10(2j-1)}}\,. \tag{67}$$

The other two points are obtained by a rotation of $\frac{2}{3}\pi$ around the origin.

More precisely for $\rho \in \partial\mathcal{D}_j^{(2)}$ one has

$$\text{rank } \rho = \begin{cases} 2j \text{ for integer } j \text{ and non exceptional points}\,, & \text{(68a)} \\ 2j-1 \text{ for integer } j \text{ and exceptional points}\,, & \text{(68b)} \\ 2j-1 \text{ for half integer } j \text{ and all points}\,. & \text{(68c)} \end{cases}$$

The figs. 1 (a) and 2 (a) show the meridian sections of $\mathcal{D}_j^{(2)}$ for $j = 1, 2, 3, 4$ and $j = \frac{3}{2}, \frac{5}{2}, \frac{7}{2}$ while the figs. 1 (b) and 2 (b) show those of $\tilde{\mathcal{D}}_j^{(2)}$ for the same $j$-values. Since $L = 2$ is the only $L$ even multipole for $j = 1$ or $\frac{3}{2}$,

$$\mathcal{D}_1^{(2)} = \tilde{\mathcal{D}}_1^{(2)}\,, \qquad \mathcal{D}_{\frac{3}{2}}^{(2)} = \tilde{\mathcal{D}}_{\frac{3}{2}}^{(2)}\,. \tag{69}$$

One also proves that

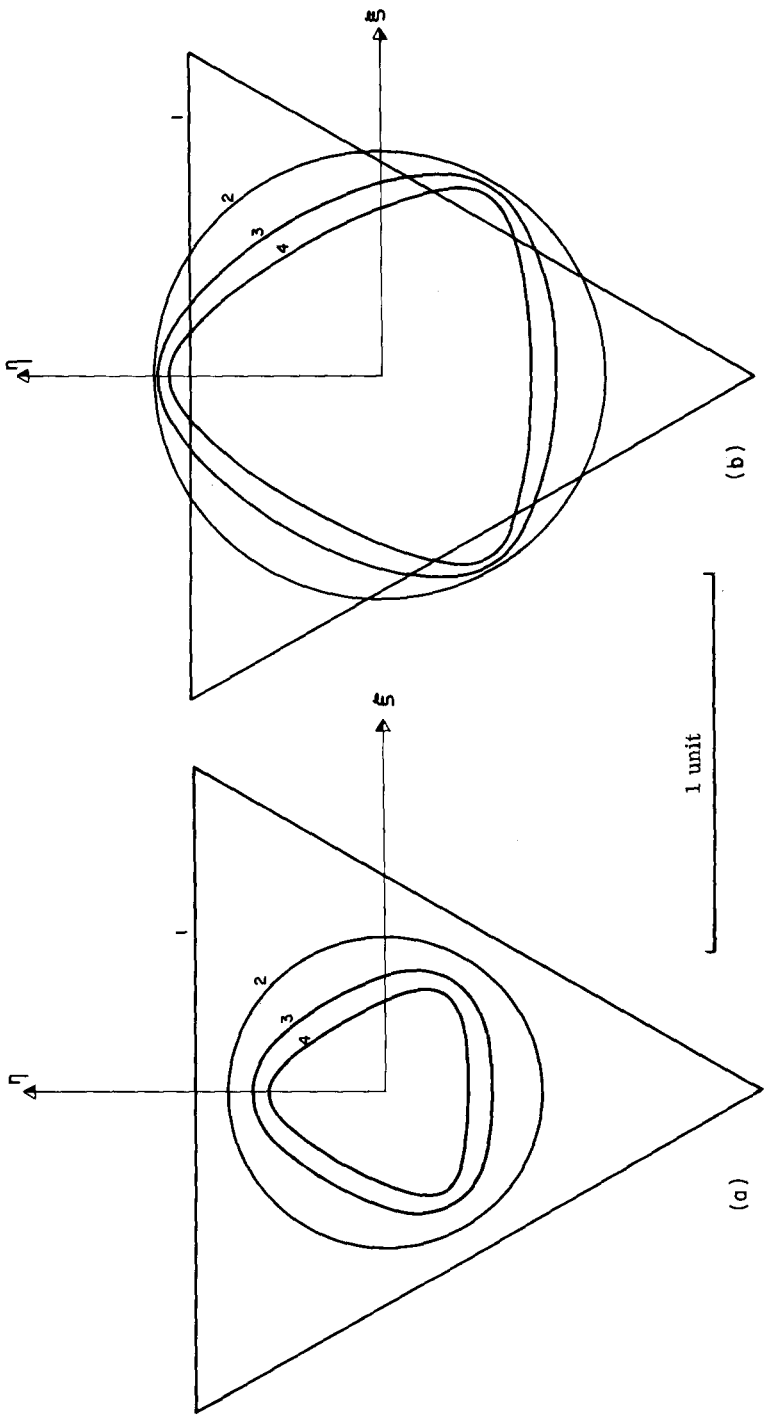


Fig. 1. Meridian sections in the two-plane $\{\xi, \eta\}$ of the five dimensional quadrupole (a) intersection $\mathcal{D}_j^{(2)}$ and (b) projection $\hat{\mathcal{D}}_j^{(2)}$, of the polarization domains $\mathcal{D}_j$ for the integer values of $j$ indicated in the figure.

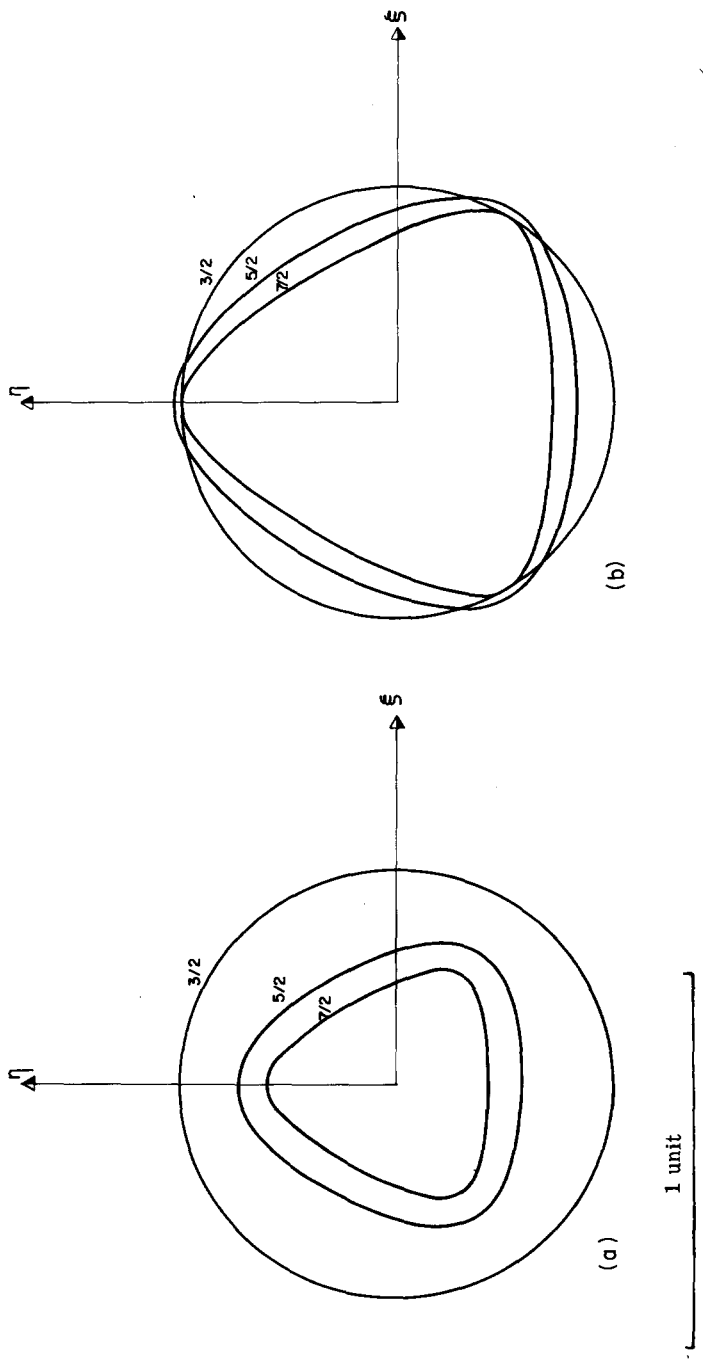


Fig. 2. Meridian sections in the two-plane $\{\xi, \eta\}$ of the five dimensional quadrupole (a) intersection $\mathcal{D}_j^{(2)}$ and (b) projection $\tilde{\mathcal{D}}_j^{(2)}$, of the polarization domains $\mathcal{D}_j$ for the half-integer values of $j$ indicated on the figure. The meridian sections of the boundaries $\tilde{\mathcal{D}}_{\frac{3}{2}}^{(2)}$ and $\tilde{\mathcal{D}}_{\frac{7}{2}}^{(2)}$ are tangent at three points.

$$\mathcal{D}_j^{(2)} \supset \mathcal{D}_{j+1}^{(2)} \quad \text{for} \quad j \geq 1 , \tag{70a}$$

and

$$\mathcal{D}_j^{(2)} \supset \mathcal{D}_{j+\frac{1}{2}}^{(2)} \quad \text{for} \quad j \geq \tfrac{3}{2} . \tag{70b}$$

3.2. *Spin tests from quadrupole angular distribution*

Let us study how the results derived in the preceding sections can be used to determine the spin of a particle whose decay mode is (i) = (1), (1') or (2). We assume that one has measured some components $y_M^{(L)}$ (cf. table 2) of the normalized angular distribution $\mathcal{I}(\theta, \varphi)$, for instance all components for $L \leq L_0$. Then the procedure for spin determination is the following:

(i) The decay modes (1), (1') and (2) are parity conserving, i.e. $\lambda_i(L, j) = 0$ for $L$ odd (see eq. (35)). Thus one must first check that the angular distribution $\mathcal{I}(\theta, \varphi)$ has no odd - $L$ multipoles, i.e. $y_M^{(L)} = 0$ when $L$ is odd ‡.

(ii) If the production section is $B$-symmetric, subsect. 2.1.5. (i), one must check that the components $y_M^{(L)}$ satisfy this symmetry ‡. These $B$-symmetry conditions are:

in any transversity quantization

$$y_M^{(L)} = 0 \quad \text{for} \quad M \text{ odd} , \tag{71}$$

in any helicity quantization

$$y_M^{(L)} = (-1)^L \overline{y_M^{(L)}} . \tag{72}$$

(iii) If one has observed non-vanishing $y_M^{(L)}$ up to $L = L_0$, of course the spin value satisfies $j \geq \frac{1}{2} L_0$. In the case $L_0 > 2$, see also sect. 4. In this section we shall consider two general cases:

(a) for $L \neq 2$, one has observed all $y_M^{(L)} = 0$,

(b) for $L \neq 2$, no information on the $y_M^{(L)}$ is known or taken into account.

Case (a), which implies an infinite number of known values of $y_M^{(L)}$, has of course much more information content than case (b), which is expected to have little power as spin test.

(iv) Compute the coordinates $\lambda\xi$, $\lambda\eta$ of $\hat{y}$, one of the points in the two-plane of meridian sections which corresponds to $y$, the point of $\mathcal{Y}^{(2)}$ re-

‡ If this is not satisfied, this simple analysis should not be carried through. Most likely, the presence of non expected $Y_M^{(L)}$ in the decay angular distribution reveals the existence of interference between the resonance channel and the background. In that case a more complete analysis is needed, e.g. ref. [2] 3.1.

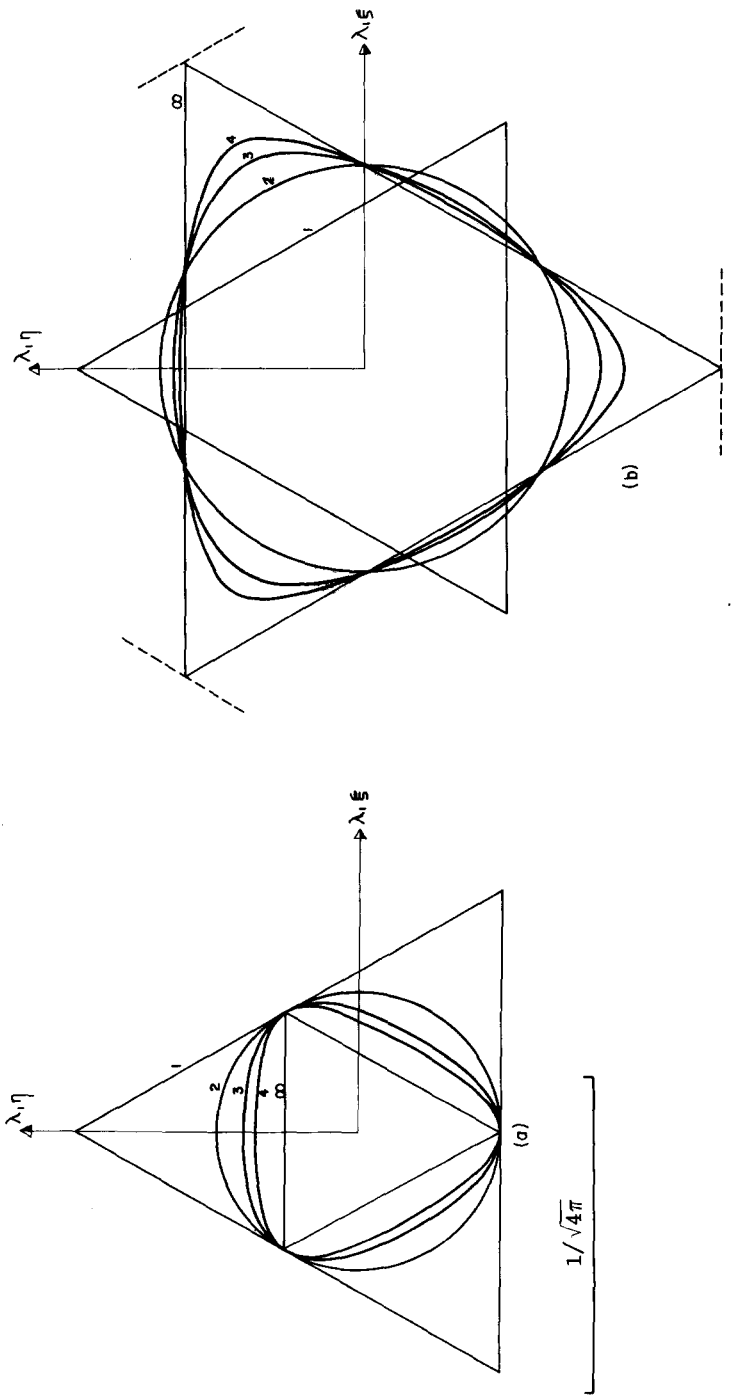


Fig. 3. Meridian sections in the two-plane $\{\lambda_1\xi, \lambda_1\eta\}$ of the five dimensional quadrupole (a) intersection $\lambda_1 \mathcal{D}_j^{(2)}$ and (b) projection $\lambda_1 \tilde{\mathcal{D}}_j^{(2)}$ for the two body decay (1) $[j \to 0 + 0]$, for the integer values of $j$ indicated in the figure. The limit $j \to \infty$ is also shown. In (a) the quadrupole *intersection* $\Delta^{(2)}$ of the *positive angular distribution* domain $\Delta$ coincide with $\lambda_1 \mathcal{D}_1^{(2)}$. In (b), only a small part of the boundary of $\tilde{\Delta}^{(2)}$, the quadrupole projection of $\Delta$, is drawn (dashed line). Note that in fig. (a), the meridian sections of all boundaries $\lambda_1 \partial \mathcal{D}_j^{(2)}$ have three common points.

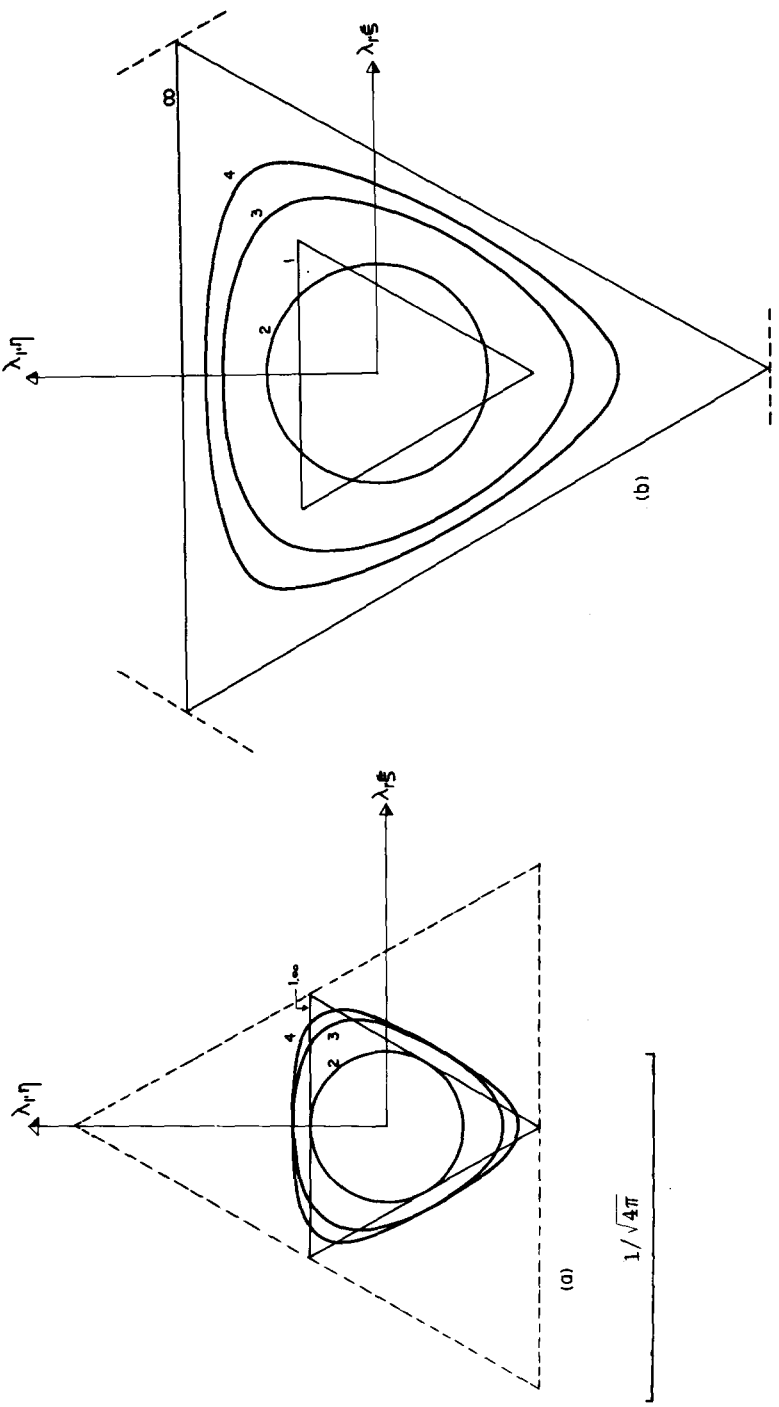


Fig. 4. Meridian sections in the two-plane $\{\lambda_1, \xi, \lambda_1, \eta\}$ of the five dimensional quadrupole (a) intersection $\lambda_1, \mathcal{D}_j^{(2)}$ and (b) projection $\lambda_1, \mathcal{D}_j^{(2)}$ for the two body decay (1') $[j^\eta \to 1^{\eta_1} + 0^{\eta_0}$, with $\eta\eta_1\,\eta_0 = (-1)^j]$, for the integer values of $j$ indicated in the figure. The dotted triangle of (a) is the meridian section of $\Delta^{(2)}$. Only a small part of that of $\tilde{\Delta}^{(2)}$ is drawn in (b). Note $\lambda_1, \mathcal{D}_1^{(2)}$ $\lambda_1, \mathcal{D}_\infty^{(2)}$.

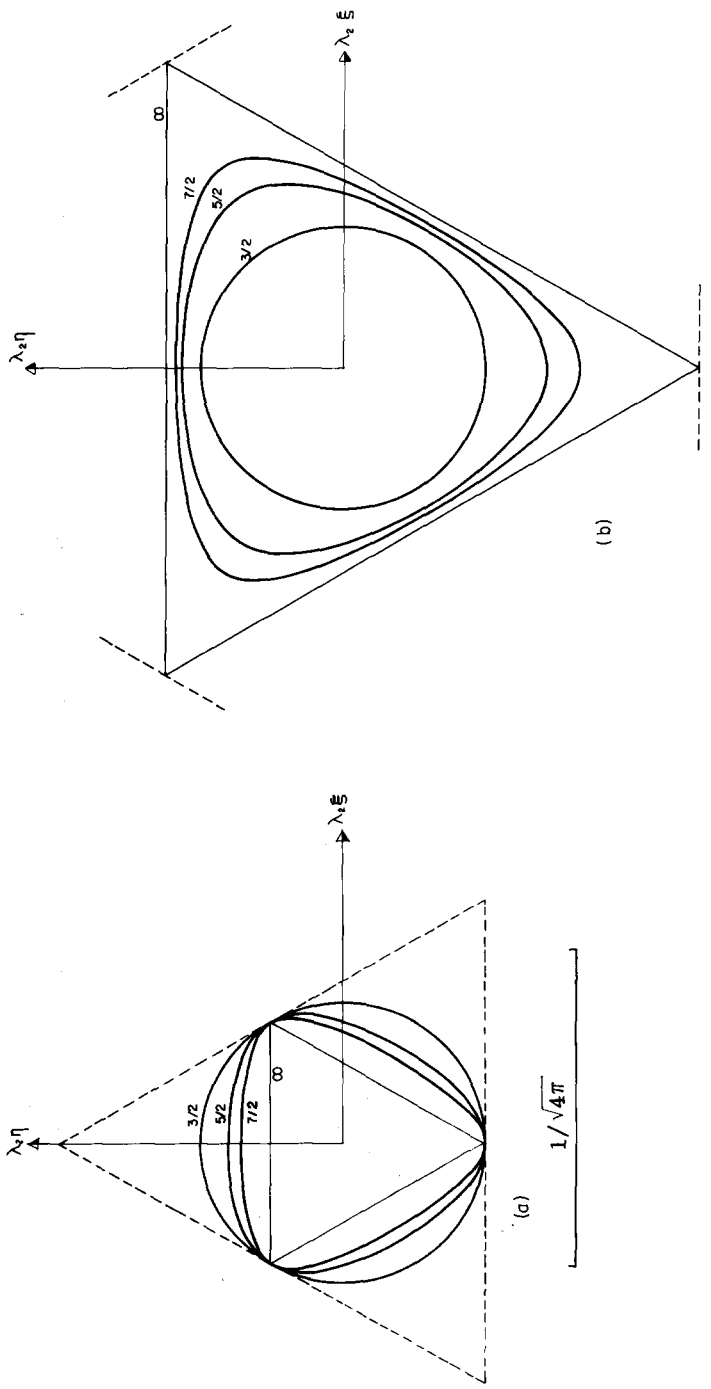


Fig. 5. Meridian sections in the two-plane $\{\lambda_2\,\xi,\ \lambda_2\,\eta\}$ of the five dimensional quadrupole (a) intersection $\lambda_2 \mathcal{D}_j^{(2)}$ and (b) projection $\lambda_2 \widetilde{\mathcal{D}}^{(2)}$ for the two body decay $\overset{(2)}{D} [j \to \frac{1}{2} + 0]$, for the half-integer values of $j$ indicated in the figure. The dotted triangle in (a) is the meridian section of $\Delta^{(2)}$. Only a small part of that of $\Delta^{(2)}$ is drawn in (b). Note that in (a), all meridian sections have three common points.

presenting the experimental data. In the general case use eqs. (54) to (57). For $B$-symmetric production reactions, when a transversity quantization has been choosen one may use eqs. (62) and for helicity quantization (63).

(v) Check that $\hat{y}$ belongs to the meridian section

(a) of $\Delta^{(2)}$, the quadrupole intersection of $\Delta$,

(b) of $\breve{\Delta}^{(2)}$, the quadrupole projection of $\Delta$,

where $\Delta$ is the domain of positive angular distributions ‡.

These meridian sections are the dotted triangles of fig. 6. The meridian section of $\Delta^{(2)}$ is also drawn in each of the figs. 3 (a), 4 (a), 5 (a), while that of $\breve{\Delta}^{(2)}$ is only suggested in the corresponding figs. 3 (b), 4 (b), 5 (b).

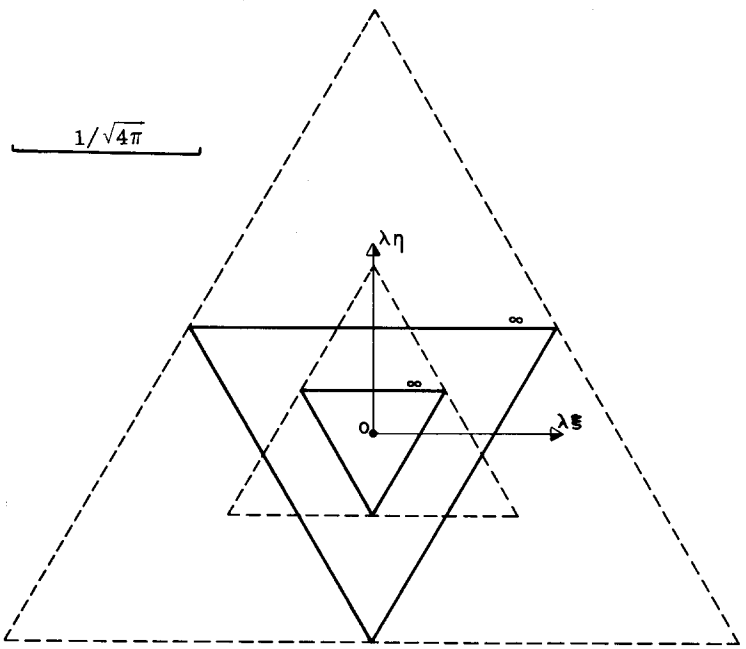


Fig. 6. These four triangles are common to figs. 3, 4, 5. The meridian sections of $\Delta^{(2)}$ and $\breve{\Delta}^{(2)}$ are the small and large deshed-line triangles respectively. Those of $\lambda\mathcal{D}_{\infty}^{(2)}$ and $\lambda\breve{\mathcal{D}}_{\infty}^{(2)}$ are the small and large solid-line triangles.

(vi) Study the relative position of $\hat{y}$ with respect to the meridian sections

(a) of the quadrupole intersections $\lambda_i \mathcal{D}_j^{(2)}$,

(b) of the quadrupole projections $\lambda_i \breve{\mathcal{D}}_j^{(2)}$,

‡ If not, this proves that the observed $y_M^{(2)}$ do correspond to a non positive angular distribution. One precedure which might yield such a distribution is to measure $g(\theta, \varphi)$ only for a limited domain of $(\theta, \varphi)$, and ask a computer to extrapolate on the whole $(\theta, \varphi)$ range by a best fit method, without imposing $g(\theta, \varphi)$ to be positive.

of the $j$-dependent polarization domain $\mathcal{D}_j$, mapped into the space of angular distribution, for the decay mode (i). These meridian sections are shown, for decay (1) in fig. 3, for decay (1') in fig. 4 and for decay (2) in fig. 5.

We now apply this study to each decay mode separately.

3.2.1. Decay mode (1): $j \to 0 + 0$.

*Case* (a)

(i) The meridian section of $\lambda_1 \mathcal{D}_j^{(2)}$ for integers $j = 1, 2, 3, 4, \infty$, are drawn in fig. 3 (a). Note that $\Delta^{(2)} = \lambda_1 \mathcal{D}_1^{(2)}$, so the experimental point $\hat{y}$ must be inside the large triangle. We have the inclusion property:

$$\lambda_1 \mathcal{D}_1 \supset \ldots \supset \lambda_1 \mathcal{D}_1^{(2)} \supset \lambda_1 \mathcal{D}_{j+1}^{(2)} \supset \ldots \supset \lambda_1 \mathcal{D}_\infty^{(2)} . \tag{73}$$

The limit $\lambda_1 \mathcal{D}_\infty^{(2)}$ is the small triangle.

All meridian sections of $\lambda_1 \mathcal{D}_j^{(2)} (j = 1, 2, \ldots, \infty)$ have three points in common on the symmetry axes; they are the middle of the sides of the large triangle. This reflects the property of the domains $\lambda \mathcal{D}_j^{(2)}$ to be tangent along the two-dimensional orbit corresponding to these three points (subsect. 3.1.2).

(ii) If there are no rank conditions on the density matrices, and if $y \in \lambda_1 \mathcal{D}_\infty^{(2)}$, no value of $j$ is excluded; if $y \notin \lambda_1 \mathcal{D}_\infty^{(2)}$, then $j \leqslant j_0$, where $j_0$ is defined by $y \notin \lambda_1 \mathcal{D}_j^{(2)}$ for $j > j_0$, and $y \in \lambda_1 \mathcal{D}_j^{(2)}$ for $j \leqslant j_0$.

The existence of $j_0$ is guaranteed by eq. (73).

In practice, due to its limited precision, the value of the experiment as spin test depends on the position of $y$ outside $\lambda_1 \mathcal{D}_\infty^{(2)}$. If $\hat{y}$ is near one of the points common to all domains, the experiment has no potential power as spin test. If $\hat{y}$ is far from these points, there is a hope to exclude spin values, and a great incentive for more precise experiments.

In fig. 3 (a) there is a large region inside the large triangle, but outside the circle which implies $j = 1$. For instance, in a $B$-symmetric experiment with a pure quadrupole decay angular distribution, the positivity domain $\Delta^{(2)}$ of this distribution is a three dimensional cone of revolution whose axis is $\lambda\eta$ and meridian section is the triangle. If the experimental point representing this angular distribution is outside the inscribed sphere (whose meridian section is that of $\lambda_1 \mathcal{D}_2^{(2)}$) then $j = 1$. Another way to say it is the following: a pure quadrupole angular distribution for this decay suggests (but does not prove!) the hypothesis $j = 1$. If the polarization analysis is made with this hypothesis, and shows a polarization degree $d_p > \frac{1}{2}$, then the hypothesis is proved.

(iii) If there is a rank condition, the experiment becomes more powerful as spin test. As we saw in subsect. 2.2 for unpolarized target and unobserved polarization of the final baryon, the strongest experimental rank condition is for reactions of the type (14)

$$0^- + \tfrac{1}{2}^+ \to j + \tfrac{1}{2} \,. \tag{74}$$

Then the polarization density matrix $\rho(j)$ of the final meson has rank $r \leqslant 4$. Its even polarization part has rank $r \leqslant 8$. When this even polarization is purely quadrupolar, condition (68a, 68b) shows that

for $2j+1 \leqslant 8$ i.e. $j = 1, 2, 3$ $y$ must be inside $\lambda_1 \mathcal{D}^{(2)}_j$ ,

for $2j = 8$ i.e. $j = 4$ $y$ must be on the boundary $\lambda_1 \mathcal{D}^{(2)}_4$ ,

and $j \geqslant 5$ is excluded by the rank condition .

To summarize: in a two body decay $j \to 0 + 0$ of a meson produced in reaction of the type (74) with a pure quadrupole angular distribution, one has $1 \leqslant j \leqslant 4$ ‡.

*Case* (b). The point $y$ cannot correspond to a positive angular distribution if it falls outside $\tilde{\Delta}^{(2)}$, the large dotted triangle of fig. 6 which is too large to be fully drawn in fig. 1 (b). Angular momentum conservation restricts much more the domain of possible $y$. It is the union of all $\lambda_1 \tilde{\mathcal{D}}^{(2)}_j$.

There is no rank condition in all cases (b) since we have made an arbitrary projection on $\mathcal{E}^{(2)}$. It is surprising that there still exists small regions compatible only with spin-one: the neighborhood of the vertices of the triangle $\lambda_1 \mathcal{D}^{(2)}_1 = \lambda_1 \tilde{\mathcal{D}}^{(2)}_1$. Near the vertices of the traingle $\lambda_1 \tilde{\mathcal{D}}^{(2)}_\infty$, there is a lower bound $j_0$ for $j$ larger than unity.

3.2.2. Decay mode (1'): $j^\eta \to 1^{\eta_1} + 0^{\eta_0}$, $\eta\eta_1\eta_0 = (-1)^j$.

*Case* (a). The domains $\lambda_1, \mathcal{D}^{(2)}_j$ are much smaller than $\Delta^{(2)}$, whose meridian section is the dotted line triangle (fig. 4 (a)) which must contain $\hat{y}$. Angular momentum conservation imposes in this case stricter conditions than the positivity of the angular distribution. This decay is a poorer spin test than the decay (1). Note that $\lambda_1, \mathcal{D}^{(2)}_1 = \lambda_1, \mathcal{D}^{(2)}_\infty$. If $\hat{y}$ is inside the circle, no value of $j$ is excluded; if it is outside, $j = 2$ is excluded. See fig. 4 (a) for more details. The rank condition depends only on the production of the resonance and not on its decay; they are therefore similar to subsect. 3.2.1 (iii).

*Case* (b). Most of the regions inside $\lambda_1, \tilde{\mathcal{D}}^{(2)}_\infty$ are compatible only with a lower spin limit $j_0$, which depends on the region, with the exception of the three corners of $\lambda_1, \tilde{\mathcal{D}}^{(2)}_1$ lying outside the sphere $\lambda_1, \tilde{\mathcal{D}}^{(2)}_2$: there, all possible integer values of $j$ are possible, except $j = 2$.

‡ The rank condition is practically lost when one integrates over a too large domain of a variable (e.g. too large "bins") or folds down the data arbitrarily.

3.2.3. Decay mode (2): $j \to \frac{1}{2} + 0$.

*Case* (a). The $\lambda_2 \mathcal{D}_j^{(2)}$ also satisfy the inclusion condition

$$\lambda_2 \mathcal{D}_{\frac{3}{2}}^{(2)} \supset \lambda_2 \mathcal{D}_{\frac{5}{2}}^{(2)} \supset \ldots \supset \lambda_2 \mathcal{D}_j^{(2)} \supset \lambda_2 \mathcal{D}_{j+1}^{(2)} \supset \ldots \supset \lambda_2 \mathcal{D}_\infty^{(2)} . \quad (75)$$

They are inside the sphere $\lambda_2 \mathcal{D}_{\frac{3}{2}}^{(2)}$ which is inscribed in $\Delta^{(2)}$ (see fig. 5 (a)). Without rank condition each region inside this sphere corresponds to a lower limit $j_0$ of $j$. All $\lambda_2 \mathcal{D}_j^{(2)}$ are tangent along the same two-dimensional orbit that the domains $\lambda_1 \mathcal{D}_j^{(2)}$ ($j$ integer, cf. fig. 3 (a)). So in fig. 5 (a) the middle of the sides of the dotted triangle are common to all domain, and if $\hat{y}$ is in their neighborhood, the experiment is not useful for spin test.

Rank condition is very important. For unpolarized target, the stricter condition appears in reactions of the type (15):

$$0^- + \tfrac{1}{2}^+ \to 0 + j . \quad (76)$$

Indeed the polarization density matrix $\rho(j)$ of the unknown spin baryon has rank $r \leqslant 2$ (see subsect. 2.1.5), its even polarization part has rank $r \leqslant 4$ (see subsect. 2.1.7). Then eq. (68c) yields that:

In a two body decay $j \to \frac{1}{2} + 0$, of a baryon produced in a reaction of the type (76), with a pure quadrupole angular distribution, the baryon spin can be only $j = \frac{3}{2}$ or $j = \frac{5}{2}$.

For $j = \frac{3}{2}$ the experimental point $\hat{y}$ can be anywhere inside the circle. For $j = \frac{5}{2}$, $\hat{y}$ must be on the drawn curve.

*Case* (b). Since $\lambda_2 \tilde{\mathcal{D}}_j^{(2)} \subset \lambda_2 \tilde{\mathcal{D}}_{j+1}^{(2)}$, each region inside $\lambda_2 \tilde{\mathcal{D}}_\infty^{(2)}$ imposes only a lower limit $j_0$ to the spin.

3.2.4. Table 3 gives the equations of all curves drawn in the figures quoted in this section. Fig. 3 (a) and 5 (a) are very similar. This is due to the following: each meridian section of $\Delta^{(2)}$, of $\lambda_1 \mathcal{D}_j^{(2)}$ and $\lambda_2 \mathcal{D}_j^{(2)}$, ($j$ integer, $j'$ half-integer $> \frac{1}{2}$) has two points on each symmetry axis. One point is common to *all* meridian sections; its ordinate on the $\lambda\eta$ axis is

$$\lambda\eta = -1/\sqrt{5} . \quad (77)$$

The ordinate of the other point is, respectively

$$\eta_j = \frac{j+1}{2j-1} \frac{1}{\sqrt{5}}, \qquad \eta_{j'} = \frac{2j'+3}{4j'} \frac{1}{\sqrt{5}}, \quad (77')$$

we remark that

$$\eta_{j'} = \eta_{j-\frac{1}{2}} . \quad (78)$$

Table 3
Equations of the curves in the figures of sect. 3.

(a) Figs. 1 (a), 2 (a) ... 5 (a) show the part of the algebraic curves $\varphi_j(\xi, \eta, \mu) = 0$ which bounds the minimal convex domain containing the origin $\xi = \eta = 0$. The homogeneity parameter $\mu$ represents unity for figs. 1 and 2, and $\lambda_i(2, j)/\lambda_i$, with the numerical value of $\lambda_i(2, j)$ given in table 1, for figs. 3, 4 and 5. As function of the invariants

$$\alpha = \xi^2 + \eta^2 , \qquad \beta = \eta(\eta^2 - 3\xi^2) ,$$

the curves $\varphi_j(\xi, \eta) = 0$ are

$$\varphi_1(\xi, \eta) = \beta + \tfrac{3}{2}\mu\alpha - \tfrac{1}{2}\mu^3 = (\eta - \tfrac{1}{2}\mu)(\eta + \sqrt{3}\xi + \mu)(\eta - \sqrt{3}\xi + \mu) ,$$

$$\varphi_2(\xi, \eta) = \alpha - \tfrac{7}{40}\mu^2 = 0 ,$$

$$\varphi_3(\xi, \eta) = 250(\alpha^3 - \beta^2) + 450\sqrt{2}\mu\alpha\beta - 465\mu^2\alpha^2 - 44\sqrt{2}\mu^3\beta + 84\mu^4\alpha - 4\mu^6$$

$$= (10\xi^2 + 2\sqrt{2}\mu\eta - \mu^2)(-5(\eta\sqrt{3} + \xi)^2 + 2\sqrt{2}\mu\eta - 2\sqrt{6}\mu\xi$$

$$+ 2\mu^2)(-5(\eta\sqrt{3} - \xi)^2 + 2\sqrt{2}\mu\eta + 2\sqrt{6}\mu\xi + 2\mu^2) = 0 ,$$

$$\varphi_4(\xi, \eta) = \beta - \tfrac{39}{40}\sqrt{\tfrac{11}{14}}\mu\alpha + \tfrac{11}{1280}\sqrt{\tfrac{77}{2}}\mu^3 = 0 ,$$

$$\varphi_{\frac{3}{2}}(\xi, \eta) = \alpha - \tfrac{1}{3}\mu^2 = 0 ,$$

$$\varphi_{\frac{5}{2}}(\xi, \eta) = \beta - 3(\tfrac{7}{10})^{\frac{3}{2}}\mu\alpha + \tfrac{2}{5}(\tfrac{7}{10})^{\frac{3}{2}}\mu^3 = 0 ,$$

$$\varphi_{\frac{7}{2}}(\xi, \eta) = 35\alpha^2 + \frac{64}{\sqrt{3}}\mu\beta - 42\mu^2\alpha + 3\mu^4 = 0 .$$

(b) The figs. 1 (b), 2 (b) ... 5 (b) are obtained from figs. 1 (a), 2 (a) ... 5 (a) by means of a polar transformation with respect to the circle

$$\xi^2 + \eta^2 + \frac{1}{2j}\mu^2 = 0 .$$

We recall that the coordinates of the points of $\psi_j(\xi', \eta'; \mu) = 0$, the polar tranform curve of $\varphi_j(\xi, \eta; \mu) = 0$, are given by:

$$\xi' = \frac{\mu}{2j}\frac{\partial\varphi}{\partial\xi}\Big/\frac{\partial\varphi}{\partial\mu} , \qquad \eta' = \frac{\mu}{2j}\frac{\partial\varphi}{\partial\xi}\Big/\frac{\partial\varphi}{\partial\mu} .$$

(c) The triangles in fig. 6 are common to figs. 3, 4 and 5. They are given by $\varphi_1(\xi, \eta; \mu) = 0$ with $\mu$ respectively

$$\sqrt{4\pi}\,\mu = \frac{1}{\sqrt{5}\lambda_i} , \frac{\sqrt{5}}{2\lambda_i} \text{ for the solid-line triangles} ,$$

$$\sqrt{4\pi}\,\mu = -\frac{2}{\sqrt{5}\lambda_i} , -\frac{\sqrt{5}}{\lambda_i} \text{ for the dashed-line triangles} .$$

The former triangles are polar tranformed of each other with respect to the circle

$$(\lambda_i\xi)^2 + (\lambda_i\eta)^2 + \frac{1}{16\pi} = 0$$

(which is that defined in (b) for the limit $j \to \infty$), and the latter triangles, with respect to the circle

$$(\lambda_i\xi)^2 + (\lambda_i\eta)^2 + \frac{1}{4\pi} = 0 .$$

## 4. POLAR ANGLE DISTRIBUTION FOR TWO-BODY DECAYS

When non vanishing multipoles $y_M^{(L)}$ are observed for $L$ up to $L_0$ and $L_0 > 2$, a complete study of the polarization domains, like that of sect. 3 for $L_0 = 2$, turns out to be very cumbersome. Indeed, the number of invariants under the "rotation" group for

$$\mathcal{Y}_{L_0} = \bigoplus_{L=1}^{L_0} \mathcal{Y}^{(L)}, \qquad \mathcal{Y}^{(E)}_{L_0} = \bigoplus_{\text{even } L=2}^{L_0} \mathcal{Y}^{(L)}, \tag{79}$$

the angular distribution spaces for general and parity conserving two body decays, are respectively:

$$\nu_{L_0} = L_0^2 + 2L_0 - 3, \qquad \nu^E_{L_0} = \tfrac{1}{2}L_0^2 + \tfrac{3}{2}L_0 - 3. \tag{80}$$

Thus for the simplest case the orbit space has dimension $\nu_4^{(E)} = 11$, to be compared with $\nu_2^{(E)} = 2$ as computed in eq. (53).

Let us therefore study in this section the simpler projections of $\mathcal{Y}_{L_0}$ and $\mathcal{Y}^{(E)}_{L_0}$ on $\mathcal{Y}^{(D)}$, the $L_0$-plane, spanned by the axes

$$Y_0^{(L)}(\theta, \varphi) = [(2L+1)\,4\pi]^{\frac{1}{2}} P_L(\cos\theta). \tag{81}$$

This plane depends on the choice of polar axis. Indeed it corresponds to the experimental measurement of the two-body decay distribution in the polar angle $\theta$, with respect to an arbitrary polar axis. This measurement supplies information only on the diagonal elements of the density matrix, and for the strong interaction decays (1), (1'), (2) only on its even part. This partial information can be however powerful as spin test.

### 4.1. *Geometry of diagonal matrix domains*

4.1.1. Let us consider the $2j$-dimensional Euclidean space $\mathcal{E}^{(D)} \subset \mathcal{E}_N$ of all diagonal, Hermitean (i.e. real), trace-one matrices. It is an equatorial $2j$-plane for the polarization domain $\mathcal{D}_j$ (cf. subsect. 2.1.7), whose intersection as well as projection can be called

$$\mathcal{D}_j^{(D)} = \mathcal{D}_j \cap \mathcal{E}^{(D)} = P_D\, \mathcal{D}_j. \tag{82}$$

The geometrical shape of $\mathcal{D}_j^{(D)}$ is a "*regular simplex*", with $n = 2j+1$ vertices and

$$n_k = \binom{n}{k} \equiv \frac{n!}{k!\,(n-k)!} \tag{83}$$

equal, $k$-dimensional faces. The $n$ vertices, $P_m$ (with $-j \leq m \leq j$), represent pure states with $\rho_{m,m} = 1$ as only non vanishing density matrix element. According to the metric in eq. (9), the vertices $P_m$ are at a distance

$d = 1$ from the unpolarized state $\rho_0$ and at a distance $l = [(2j+1)/j]^{\frac{1}{2}}$ from each other.

4.1.2. Among the many symmetries of $\mathcal{D}_j^{(D)}$, we are interested in its symmetry through $\mathcal{E}^{(E)}$, the *even-L polarization* plane (cf. subsect. 2.1.6). Since this symmetry permutes the vertices $P_m$ and $P_{-m}$, $\mathcal{E}^{(E)}$ is a "mediatrix" plane for all the edges $P_m P_{-m}$, and contains the vertex $P_0$ when it exists, i.e. when $j$ is integer. For this symmetry plane projection and intersection coincide too:

$$\mathcal{D}_j^{(D,E)} = \mathcal{D}_j^{(D)} \cap \mathcal{E}^{(E)} = P_E \mathcal{D}_j^{(D)} . \tag{84}$$

In the case of half-integer $j$, the domain $\mathcal{D}_j^{(D,E)}$ is another regular simplex, whose vertices, $P'_m (\frac{1}{2} \leq m \leq j)$, are placed at the middle of the edges $\overline{P_m P_{-m}}$ of $\mathcal{D}_j^{(D)}$. Its dimension if $j - \frac{1}{2}$, and each of its $n' = j + \frac{1}{2}$ vertices lies at a distance $d' = [(2j-1)/4j]^{\frac{1}{2}}$ from $\rho_0$, and at a distance $l' = [(2j+1)/2j]^{\frac{1}{2}}$ from each other.

In the case of integer $j$, the simplex $\mathcal{D}_j^{(D,E)}$ has $n'' = j+1$ vertices, and its dimension is $j$, but it is no longer regular. Each of the $j$ vertices $P'_m$ $(1 \leq m \leq j)$ lies also at a distance $d'' = d'$ from $\rho_0$ and at a distance $l'' = l'$ from each other. But the singular vertex $P_0$ is at a distance $d''_0 = 1$ from $\rho_0$ and at a distance $[3(2j+1)/4j]^{\frac{1}{2}}$ from the others. These metrical properties of $\mathcal{D}_j^{(D)}$ and $\mathcal{D}_j^{(D,E)}$ are summarized in table 4.

Since $\mathcal{E}^{(D)}$ and $\mathcal{E}^{(D,E)}$ are equatorial planes of $\mathcal{D}_j$, the simplices $\mathcal{D}_j^{(D)}$ and $\mathcal{D}_j^{(D,E)}$ are self transformed by a polar transformation with respect to the sphere of radius $R = [-1/2j]^{\frac{1}{2}}$ centered at $\rho_0$ (cf. subsect. 2.1.8).

Table 4

Polarization domains $\mathcal{D}_j^{(D)}$ and $\mathcal{D}_j^{(D,E)}$ for diagonal and diagonal even density matrices of spin $j$. Their geometrical shape is a $(n-1)$-dimensional simplex with $n$ vertices. Each one of these vertices lies at a distance $d$ from the unpolarized state, and at a distance $l$ from each other. The simplices are regular, except for integer spin and even polarization, for which a singular vertex of the simplex lies at a distance $d_0 = 1$ from the unpolarized state and at a distance $l_0$ from the other vertices.

| (a) $j$ = half-integer | | | | (b) $j$ = integer | | | | |
|---|---|---|---|---|---|---|---|---|
| $n$ | $d$ | $l$ | | $n$ | $d$ | $l$ | $d_0$ | $l_0$ |
| $2j+1$ | 1 | $\left[\frac{2j+1}{j}\right]^{\frac{1}{2}}$ | $\mathcal{D}_j^{(D)}$ | $2j+1$ | 1 | $\left[\frac{2j+1}{j}\right]^{\frac{1}{2}}$ | | |
| $j+\frac{1}{2}$ | $\left[\frac{2j-1}{4j}\right]^{\frac{1}{2}}$ | $\left[\frac{2j+1}{2j}\right]^{\frac{1}{2}}$ | $\mathcal{D}_j^{(D,E)}$ | $j+1$ | $\left[\frac{2j-1}{4j}\right]^{\frac{1}{2}}$ | $\left[\frac{2j+1}{2j}\right]^{\frac{1}{2}}$ | 1 | $\left[\frac{3(2j+1)}{4j}\right]^{\frac{1}{2}}$ |

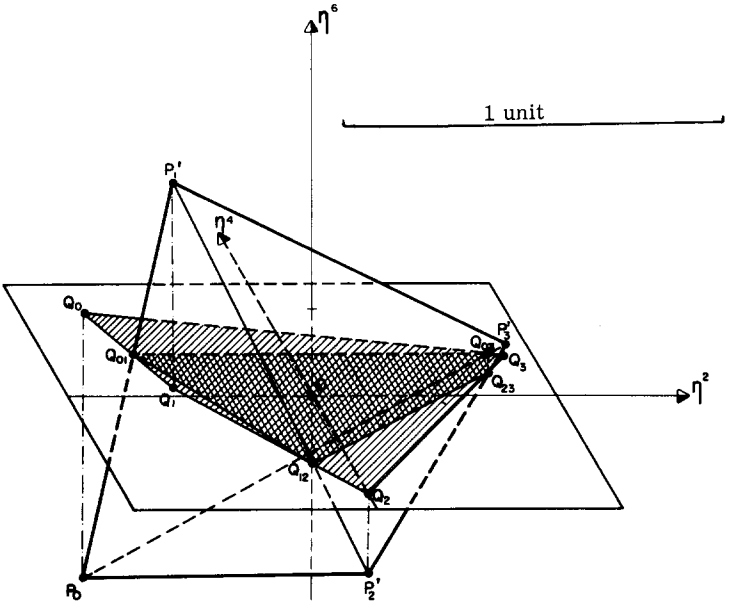


Fig. 7. The tetrahedron $P'_0P'_1P'_2P'_3$ is an example of a diagonal even polarization domain $\mathcal{D}\,^{(D,E)}_{j}$ for $j = 3$. The shaded polygones $Q_0Q_1Q_2Q_3$ and $Q_{01}Q_{12}Q_{23}Q_{03}$ are respectively the intersection with, and the projection on the two-plane $\{\eta^2, \eta^4\}$.

4.1.3. As an *illustration*, fig. 7 shows the domain $\mathcal{D}\,^{(D,E)}_{j}$ for $j = 3$. It is a regular pyramid with base $P'_1P'_2P'_3$ and apex $P_0$. According to table 4, the point 0, representative of the unpolarized state, lies on the ternary symmetry axis at distances $\frac{1}{6}$ and 1 from base and apex respectively. Point 0 lies also on the perpendicular from each vertex $P'_m$ to the opposite face at distances $[\frac{1}{15}]^{\frac{1}{2}}$ and $[\frac{5}{12}]^{\frac{1}{2}}$ from face and vertex respectively. This means that the pyramid is self transformed by a polar transformation with respect to the sphere of radius $R = [-\frac{1}{6}]^{\frac{1}{2}}$ centered at 0.

In fig. 7 are also shown the polygones $Q_0Q_1Q_2Q_3$ and $Q_{01}Q_{12}Q_{23}Q_{03}$ which constitute the projection on, and the intersection by the oblique plane $\{\eta^2, \eta^4\}$. They are consequently transformed from each other by the polar transformation induced in the plane $\{\eta^2, \eta^4\}$ with respect to the circle of radius $R$.

Such intersections and projections are respectively drawn in parts (a) and (b) of fig. 8, 9. The polygons labelled $A$, $bB$, $cC$, $dD$ in fig. 8 correspond to $j = 1, 2, 3, 4$, and those labelled $A$, $bB$, $cC$ in fig. 9, to $j = \frac{3}{2}, \frac{5}{2}, \frac{7}{2}$. The point labelled $X_m$ in part (b) of figs. 8 (or 9) is the projection of the simplex vertex representing the density matrix whose only non null elements are $\rho_{m,m}$, $\rho_{-m,-m}$ (or $\rho_{\frac{1}{2}m,\frac{1}{2}m}$, $\rho_{-\frac{1}{2}m,-\frac{1}{2}m}$). The polygons in parts (a) and (b) of these figures are polar transforms of each other, and the transform of

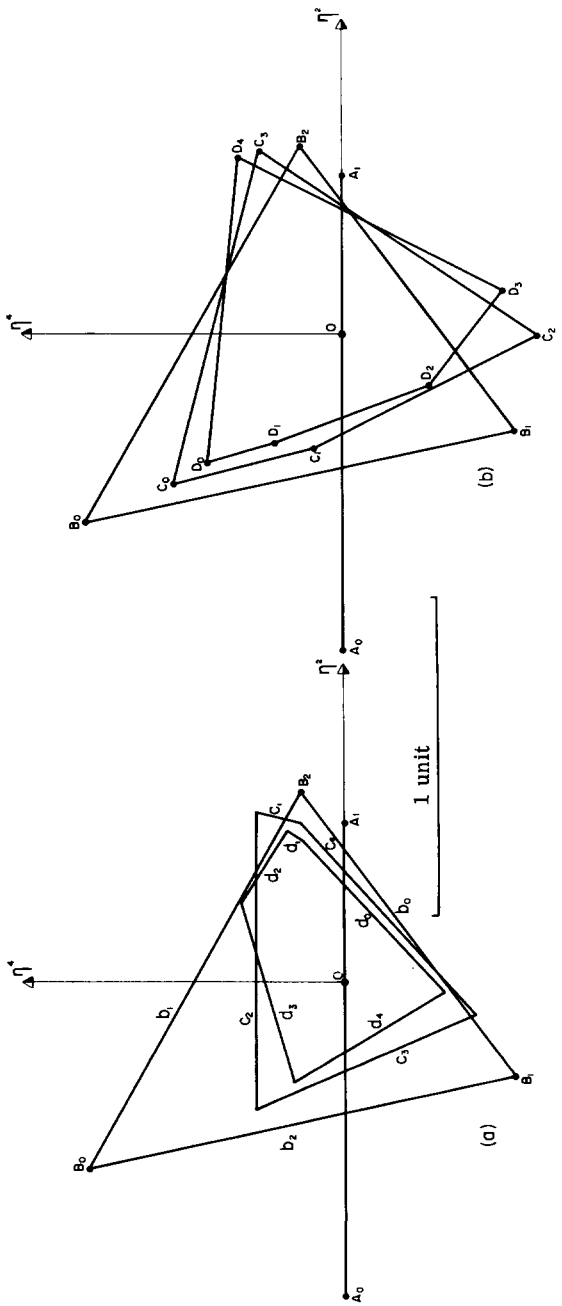


Fig. 8. (a) intersection and (b) projection of the simplices $\mathcal{D}_j^{(D,E)}$, diagonal even polarization domains, for the two plane $\{\eta^2, \eta^4\}$. The labels $A$, $bB$, $cC$, $dD$ correspond respectively to the spin values $j = 1, 2, 3, 4$. In (b) $X_m$ is the projection of the state with density matrix elements: $\rho_{00} = 1$ or, for $m \neq 1$, $\rho_{mm} = \rho_{-m,-m} = \frac{1}{2}$. Its polar transform is the segment $x_m$ in (a). For $j = 1$ and 2 the projection and intersection coincide: $A_0A_1$, $B_0B_1B_2$.

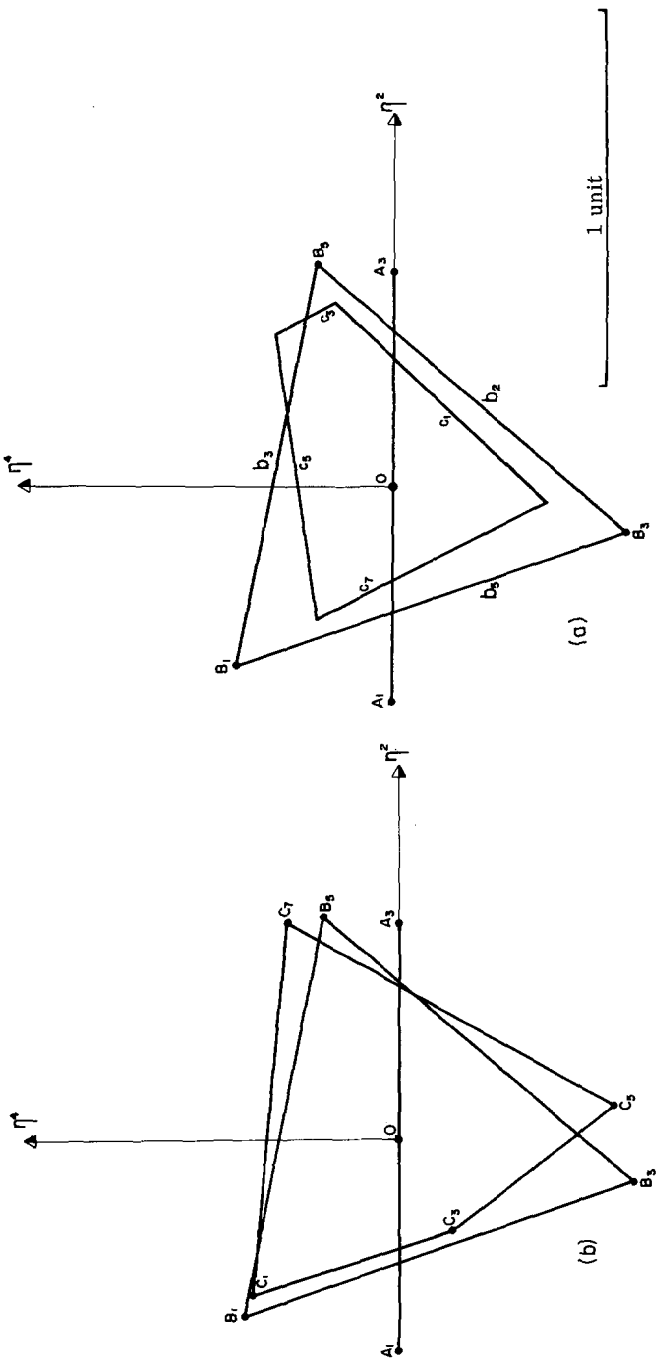


Fig. 9. (a) intersection and (b) projection of the simplices $\mathcal{D}_j^{(D,E)}$, diagonal even polarization domains, for the two plane $\eta^2$, $\eta^4$. The labels $A$, $bB$, $cC$ correspond respectively to the spin values $j = \frac{3}{2}, \frac{5}{2}, \frac{7}{2}$. In (b) $X_m$ is the projection of the state with density matrix elements $\rho_{\frac{1}{2}m, \frac{1}{2}m} = \rho_{-\frac{1}{2}m, -\frac{1}{2}m} = \frac{1}{2}$. Its polar transform is the segment $x_m$ in (a). For $j = \frac{3}{2}$ and $\frac{5}{2}$ the projection and intersection coincide: $A_1A_3$, $B_1B_3B_5$.

vertex $X_m$ in (b) is the side labelled $x_m$ in (a).

4.1.4. Conditions in the production process, like $B$-symmetry, collinearity and rank conditions (cf. subsect. 2.1.5), can reduce the domains $\mathcal{D}_j^{(D)}$ and $\mathcal{D}_j^{(D,E)}$ to different subdomains according to the choosen quantization. For instance, the planes $\mathcal{E}^{(B)}$ and $\mathcal{E}^{(B,E)}$ of *B-symmetric*, even matrices depend only on the orientation of the reaction plane, while the planes $\mathcal{E}^{(D)}$ and $\mathcal{E}^{(D,E)}$ of diagonal and even, diagonal matrices depend on the direction of the polar axis. For transversity one has

$$T_{\mathcal{E}}(D) \subset \mathcal{E}(B), \tag{85}$$

and the domains $T_{\mathcal{D}_j}^{(D)}$ and $T_{\mathcal{D}_j}^{(D,E)}$ are not reduced in the case of $B$-symmetry

$$\mathcal{E}^{(B)} \cap T_{\mathcal{D}_j}^{(D)} = T_{\mathcal{D}_j}^{(D)}, \qquad \mathcal{E}^{(B)} \cap T_{\mathcal{D}_j}^{(D,E)} = T_{\mathcal{D}_j}^{(D,E)}. \tag{85'}$$

But for helicity quantizations one has (cf. ref. [2])

$$H_{\mathcal{E}}(D) \cap \mathcal{E}^{(B)} = H_{\mathcal{E}}(D,E) \subset \mathcal{E}^{(B,E)}, \tag{86}$$

and the domain $H_{\mathcal{D}_j}^{(D)}$ reduces to $H_{\mathcal{D}_j}^{(D,E)}$ in the case of $B$-symmetry:

$$\mathcal{E}^{(B)} \cap H_{\mathcal{D}_j}^{(D)} = \mathcal{E}^{(B)} \cap H_{\mathcal{D}_j}^{(D,E)} = H_{\mathcal{D}_j}^{(D,E)}. \tag{86'}$$

Finally for a quantization axis oblique to the production plane, one has

$$O_{\mathcal{E}}(D) \cap \mathcal{E}^{(B)} = \rho_0 \tag{87}$$

and the $B$-condition reduces the domain $\mathcal{D}_j^{(D)}$ to the unpolarized state

$$\mathcal{E}^{(B)} \cap \mathcal{D}_j^{(D)} = \mathcal{E}^{(B)} \cap \mathcal{D}_j^{(D,E)} = \rho_0. \tag{87'}$$

In the case of collinear production, and helicity quantization, the density matrices are diagonal and both polarization domains coincide:

$$H_{\mathcal{E}}(D) = \mathcal{E}^{(C)}, \qquad H_{\mathcal{D}}(D) = \mathcal{D}^{(C)}. \tag{88}$$

For transversity quantization (or for any quantization axis oblique to the collinearity direction) these spaces and domains have only one common point:

$$T_{\mathcal{E}}(D) \cap \mathcal{E}^{(C)} = T_{\mathcal{D}}(D) \cap \mathcal{D}^{(C)} = \rho_0. \tag{89}$$

The *rank* of the matrices represented by points inside the simplices

$\mathcal{D}_j^{(D)}$, $\mathcal{D}_j^{(D,E)}$ is maximal, rank $\rho = 2j+1$. For points on the boundary it is strictly smaller, and simply related to the dimension $k$ of the minimal $k$-face containing $\rho$:

$$\text{rank } \rho = \begin{cases} k+1 \text{ for } \mathcal{D}_j^{(D)} ; & \text{(90a)} \\ 2k+2 \text{ for } \mathcal{D}_j^{(D,E)} \text{ with half-integer } j, \text{ or with integer } j \text{ and } k\text{-faces non containing } P_0 ; & \text{(90b)} \\ 2k+1 \text{ for } \mathcal{D}_j^{(D,E)} \text{ with integer } j \text{ and } k\text{-faces containing } P_0 . & \text{(90c)} \end{cases}$$

Rank conditions are not useful when one integrates over the azimuthal angular distribution, because this projects the polarization point on the equatorial plane $\mathcal{E}^{(D)}$. But these conditions can be powerful for instance in the case of collinear production and helicity quantization, when one knows that, according to eq. (88), the physical domain is the diagonal one. Then for reactions of type (14),

$$0^- + \tfrac{1}{2}^+ \to j + \tfrac{1}{2} , \qquad (91)$$

the density matrix $\rho(j)$ of the final meson has rank $r \leq 3$, and one knows that only its elements $\rho_{11}, \rho_{00}, \rho_{-1-1}$ can be non null. Analogously, for reactions of type (15)

$$0^- + \tfrac{1}{2}^+ \to 0^- + j , \qquad (92)$$

the $\rho(j)$ of the final baryon has rank $r \leq 2$, and only $\rho_{\frac{1}{2}\frac{1}{2}}$ and $\rho_{-\frac{1}{2}-\frac{1}{2}}$ can be non null (cf. Adair test in ref. [10]).

4.1.5. The linear mapping of the space $\mathcal{E}_N$ into the space $\mathcal{Y}$ allows to translate the considerations above to the space of *polar angle distributions* $\mathcal{Y}^{(D)}$. In particular the regular simplices $\mathcal{D}_j^{(D)}$ are mapped into simplies

$$\lambda_i(L, j)\, \mathcal{D}_j^{(D)} = \lambda_i(L, j)\, \mathcal{D}_j^{(D,E)} \qquad (93)$$

which depend on the decay mode (i) = (1), (1'), (2). The different dilations $\lambda_i(L)$, along the axes $Y_0^{(L)}$ destroy their regularity.

4.2. *Spin tests from polar angle distribution*

Let us apply the considerations of the preceding subsection to the spin determination of a particle whose decay mode is (i) = (1), (1') or (2). The analysis of the angular distribution in $\theta$, the polar angle with respect to any well defined direction, supplies the diagonal multipoles $y_0^{(L)}$ (cf. table 2), i.e. the projection, $y^{(D)}$, of the angular distribution representative

point, $y \in \mathcal{Y}$, on the polar angle distribution space $\mathcal{Y}^{(D)}$. We assume that one has measured in this way some $y_0^{(L)} \neq 0$ up to $L = L_0 > 2$, and that one has checked the parity conservation in the decay and eventually in the production processes (cf. subsect. 3.2.1 (i) and (ii)). Then the procedure for spin determination is the following:

(i) the only consequence of angular momentum conservation, for any assumed spin $j$, is that the point $y^{(D)}$ must belong to the corresponding *diagonal* polarization simplex

$$y^{(D)} \in \lambda_i(L, j)\, \mathcal{D}_j^{(D)} , \tag{94}$$

whose vertices can be obtained from table 5 (a), and from the dilation coefficients $\lambda_i(L, j)$ given in table 1. Condition (94) is equivalent to the positivity of the diagonal density matrix elements, $\rho(j)_{m,m} \geq 0$, which can be computed from the measured $y_0^{(L)}$ by means of tables 1 and 2, and eqs. (37) and (39). Condition (94) can therefore be used as spin tests in an

Table 5
Coordinates and equations for the figures of sect. 4.

(a) The coordinates of any vertex $P_m$ of the diagonal polarization simplices, like that shown in fig. 7, are:

$$\eta^L = (-)^{j-m}\, [(2L+1)\,(2j+1)/2j]^{\frac{1}{2}} \begin{pmatrix} j & j & L \\ m & -m & 0 \end{pmatrix} .$$

In particular the two coordinates for the vertex $X_m$ of the polygons $\mathcal{D}_j^{(2,4)}$ obtained by projection of these simplices in figs. 8 (b), 9 (b) ... 12 (b) are:

$$\eta^2 = -\mu^2 5^{\frac{1}{2}} j^{-1} [j(j+1) - 3m^2]\, [(2j+3)\,(2j+2)\,(2j-1)]^{-\frac{1}{2}}$$

$$\eta^4 = \mu^4 3j^{-1} [3(j+2)\,(j+1)\,j(j-1) - 5(6j^2 + 6j - 5)\, m^2 + 35m^4]$$

$$\times [(2j+5)\,(2j+4)\,(2j+3)\,(2j+2)\,(2j-1)\,(2j-2)\,(2j-3)]^{-\frac{1}{2}} .$$

For figs. 8 and 9, the parameters $\mu^L$ represent $\mu^2 = \mu^4 = 1$, and for figs. 10, 11 and 12 $\mu^L = \lambda_i(L, j)/\lambda_i^L$ with the numerical values of $\lambda_i(L, j)$ given in table 1.

(b) The polygons of the intersections $\mathcal{D}_j^{(2,4)}$ shown in figs. 8 (a), 9 (a) ... 12 (a) are obtained from those in figs. 8 (b), 9 (b) ... 12 (b), by a polar tranformation with respect to the ellipse

$$(\eta^2/\mu^2)^2 + (\eta^4/\mu^4)^2 + \frac{1}{2j} = 0 .$$

We recall that the equation of the straight line $x_m$ polar transform of the point $X_m = (\lambda^2 \eta_0^2, \lambda^4 \eta_0^4)$ is:

$$(\mu^2)^{-2}\, \eta_0^2 \eta^2 + (\mu^4)^{-2}\, \eta_0^4 \eta^4 + \frac{1}{2j} = 0 .$$

Table 5 (continued)

(c) The "parachute-shaped" domains $\mathcal{D}_{\infty}^{(2,4)}$, $\Delta^{(2,4)}$, and "bullet-shaped" domains $\tilde{\mathcal{D}}_{\infty}^{(2,4)}$, $\tilde{\Delta}^{(2,4)}$ in fig. 13 are common to figs. 10, 11, 12 (a) and (b) respectively. The "parachute-shaped" domains are bounded by the ellipse

$$18\,(\eta^4/\mu^4)^2 + 3\,(\eta^2/\mu^2)^2 - 2\sqrt{5}\,(\eta^4/\mu^4)\,(\eta^2/\mu^2) - 14\,(\eta^4/\mu^4) = 0\ ,$$

and the two segments $\overline{PT}_1$, $\overline{PT}_2$ tangent at $T_1$ and $T_2$ with

$$P = (\eta^2\sqrt{5}, -\mu^4 4/7)\ , \qquad T_1 = (-\mu^2 10/7\sqrt{5}, \mu^4/7)\ , \qquad T_2 = (\mu^2 20/7\sqrt{5}, \mu^4 8/21)\ .$$

The "bullet-shaped" domains are bounded by the parabole

$$7(\eta^2/\mu^2)^2 - 6(\eta^4/\mu^4) - 2\sqrt{5}(\eta^2/\mu^2) - 7 = 0\ ,$$

between the points

$$P_1 = (\mu^2\sqrt{5}, \mu^2 3)\ , \qquad P_2 = (-\mu^2\sqrt{5}/2, \mu^4 9/8)\ ,$$

and by the segment $\overline{P_1P_2}$.
The values of $\mu^2$, $\mu^4$ are

$\sqrt{4\pi}\,\mu^2 = -1/2\lambda_i^2$ , $\sqrt{4\pi}\,\mu^4 = 3/8\lambda_i^4$ for $\mathcal{D}_{\infty}^{(2,4)}$ , $\hat{\mathcal{D}}_{\infty}^{(2,4)}$ (solid line diagrams) ,

$\sqrt{4\pi}\,\mu^2 = 1/\lambda_i^2$ , $\sqrt{4\pi}\,\mu^4 = 1/\lambda_i^4$ for $\Delta^{(2,4)}$ , $\hat{\Delta}^{(2,4)}$ (dashed line diagrams) .

These domains $\mathcal{D}$ and $\hat{\mathcal{D}}$ and these domains $\Delta$ and $\hat{\Delta}$ are polar transform from each other with respect to the ellipse or circle

$$(\eta^2/\mu^2)^2 + (\eta^4/\mu^4)^2 = 1\ .$$

algebraic, blind way. We will propose a partial application of condition (94), which visualizes the potential power of experimental data for spin determination.

(ii) Let us distinguish two cases:

(a) one has observed all $y_0^{(L)} = 0$, for $L \neq 2, 4$;

(b) one knows only or takes only into account the measured $y_0^{(2)}$ and $y_0^{(4)}$.

Let us call in both cases $\hat{y} = (y_0^{(2)}, y_0^{(4)})$ the measured point (a) lying in or (b) projected on the plane spanned by $Y_0^{(2)}$ and $Y_0^{(4)}$, which we label $\{\lambda_i^2\eta^2, \lambda_i^4\eta^4\}$.

(iii) Check first of all the positivity of the polar angle distribution, i.e. that $\hat{y}$ belongs to

(a) the intersection of $\Delta^{(D)}$ by $\{\lambda_i^2\eta^2, \lambda_i^4\eta^4\}$;

(b) the projection of $\Delta^{(D)}$ on $\{\lambda_i^2\eta^2, \lambda_i^4\eta^4\}$.

This intersection and this projection are the "parachute-shaped" and "bullet-shaped" dotted diagrams, which are shown in fig. 13, and suggested respectively in parts (a) and (b) of figs. 10, 11 and 12.

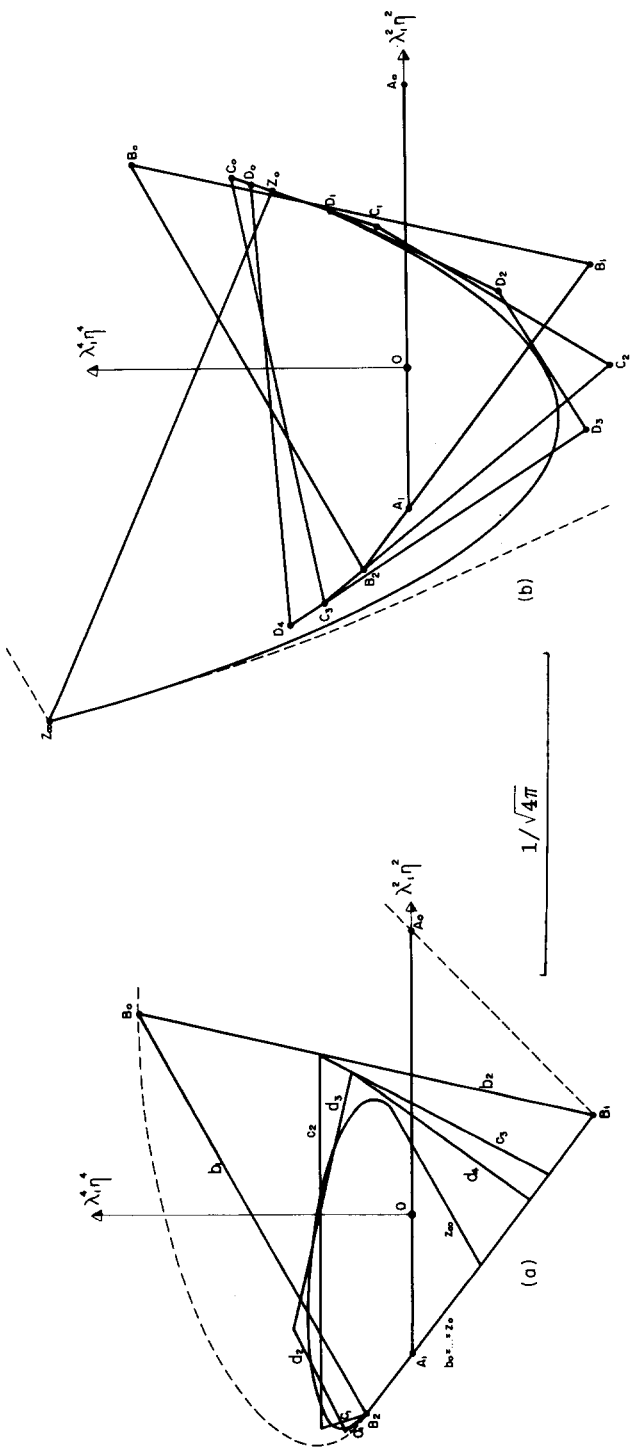


Fig. 10. For the decay mode (1) $[j \to 0\,0]$, (a) intersection and (b) projection of the simplicies $\lambda_1 (L)\, \mathcal{D}^{(D,E)}_j$, diagonal even polarization domains, for the two-plane $\{\lambda_1^2 \eta^2, \lambda_1^4 \eta^4\}$ or polar angle distribution in $Y_0^{(2)}$ and $Y_0^{(4)}$, for the $j$ values 1, 2, 3, 4 and the limit $j \to \infty$. The labels $A$, $bB$, $cC$, $dD$ correspond respectively to the spin values $j = 1, 2, 3, 4$. The labels $zZ$ correspond to the limit $j \to \infty$. The points $Z_0$ and $Z_\infty$ in (b) are projection of the states, with density matrix elements $\rho_{00} = 1$ and $\rho_{jj} = \rho_{-j-j} = \frac{1}{2}$ for $j \to \infty$. The dashed lines partially show (a) the intersection, (b) the projection of the positivity domain $\Delta^{(D)}$ of the polar angle distribution.

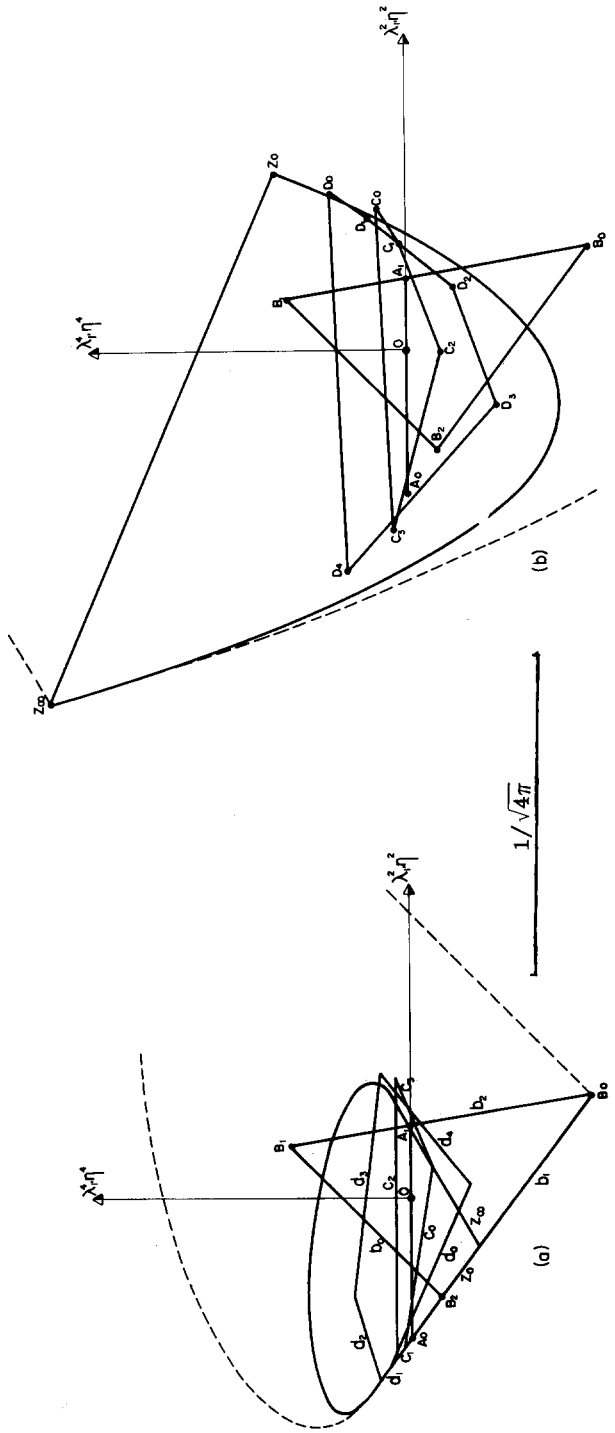


Fig. 11. For the decay mode (1') $[j \to 1\,0]$, (a) intersection and (b) projection of the simplices $\lambda_1' (L)\, \mathcal{D}_j^{(D,E)}$, diagonal even polarization domains, for the two-plane $\{\lambda_1^2 \eta^2, \lambda_1^4 \eta^4\}$ of polar angle distribution in $Y_0^{(2)}$ and $Y_0^{(4)}$, for the $j$ values 1, 2, 3, 4 and the limit $j \to \infty$. The labels $A$, $bB$, $cC$, $dD$ correspond respectively to the spin values $j = 1, 2, 3, 4$. The labels $zZ$ correspond to the limit $j \to \infty$. The points $Z_0$ and $Z_\infty$ in (b) are projection of the states, with density matrix elements $\rho_{00} = 1$ and $\rho_{jj} = \rho_{-j\,-j} = \frac{1}{2}$ for $j \to \infty$. The dashed lines partially show (a) the intersection, (b) the projection of the positivity domain $\Delta^{(D)}$ of the polar angle distribution.

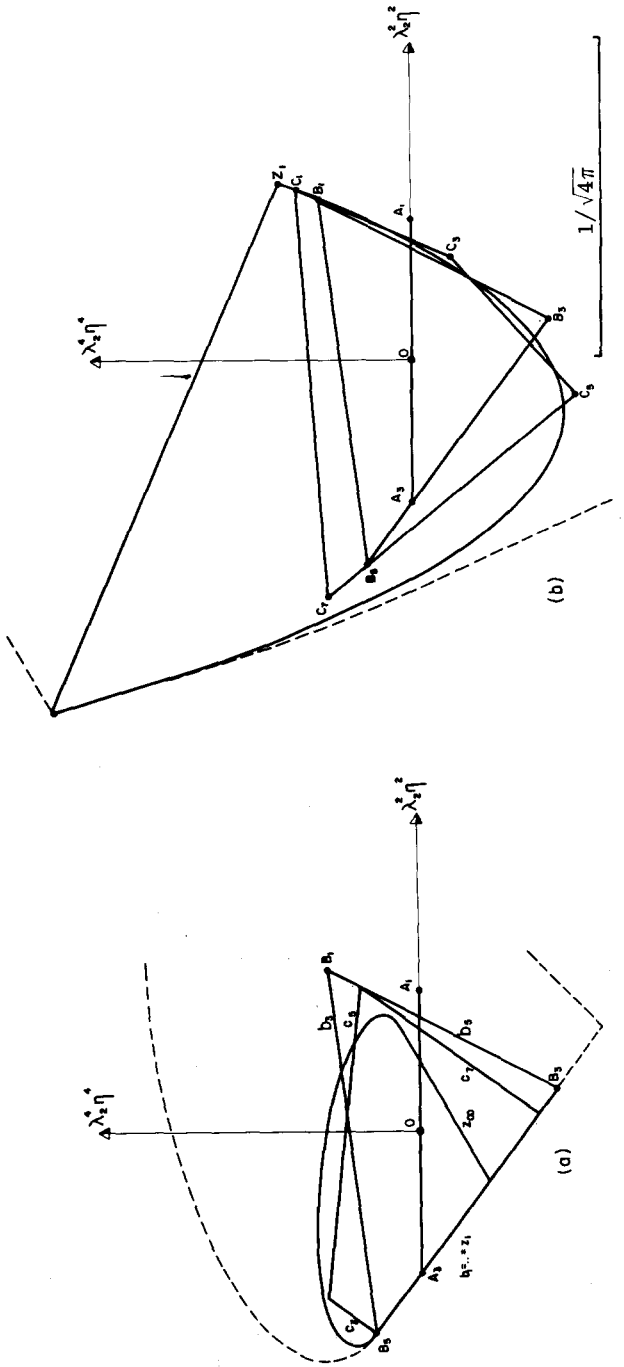


Fig. 12. For the decay mode (2) $[j \to \frac{1}{2}\,0]$, (a) intersection and (b) projection of the simplices $\lambda_2(L)\,\mathcal{D}_j^{(D,E)}$, diagonal even polarization domains, for the two-plane $\{\lambda_2^2\eta^2, \lambda_2^4\eta^4\}$ of polar angle distribution in $Y_0^{(2)}$ and $Y_0^{(4)}$, for the $j$ values $\frac{3}{2}$, $\frac{5}{2}$, $\frac{7}{2}$ and the limit $j \to \infty$. The labels $A$, $bB$, $cC$ correspond respectively to the spin values $j = \frac{3}{2}, \frac{5}{2}, \frac{7}{2}$. The labels $zZ$ correspond to the limit $j \to \infty$. The point $Z_0$ and $Z_\infty$ in (b) are projection of the states, with density matrix elements $\rho_{\frac{1}{2}\frac{1}{2}} = \rho_{-\frac{1}{2}-\frac{1}{2}} = \frac{1}{2}$ and $\rho_{jj} = \rho_{-j-j} = \frac{1}{2}$ for $j \to \infty$. The dashed lines partially show (a) the intersection, (b) the projection of the positivity domain $\Delta^{(D)}$ of the polar angle distribution.

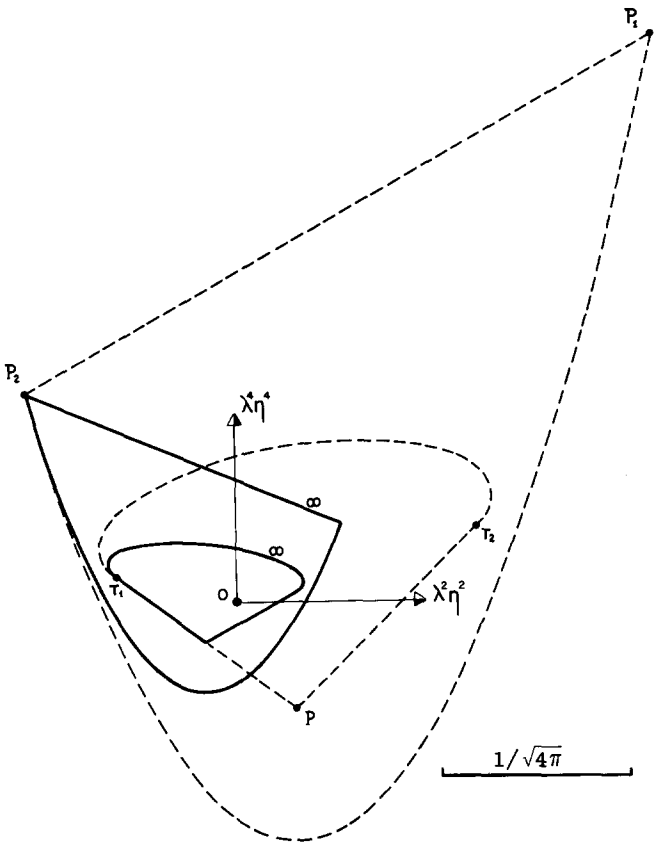


Fig. 13. The four diagrams in this figure are common to figs. 10, 11, 12. The dashed line diagrams show the "parachute-shaped" intersection and the "bullet-shaped" projection for the two plane $\lambda^2\eta^2$, $\lambda^4\eta^4$ of the positivity domain $\Delta^{(D)}$ of the polar angle distribution. The solid line diagrams are the intersection and projection of the diagonal polarization domain $\lambda\mathcal{D}_{\infty}^{(D)}$. Note that the polar transform of the points $P_1$, $P_2$ are the tangents $PT_1$, $PT_2$.

(iv) Study the relative position of $\hat{y}$ with respect to

(a) the intersection of $\lambda_i \mathcal{D}_j^{(D)}$ by $\{\lambda_i^2\eta^2, \lambda_i^4\eta^4\}$,

(b) the projection of $\lambda_i \mathcal{D}_j^{(D)}$ on $\{\lambda_i^2\eta^2, \lambda_i^4\eta^4\}$,

where $\lambda_i \mathcal{D}_j^{(D)}$ is the *j-dependent*, diagonal polarization domain, mapped into the space of angular distribution, for the decay mode (i). These intersections and projections are shown in figs. 10, 11 and 12, for decay modes (i) = (1), (1') and (2) respectively. We shall consider them separately below.

(v) Note that the procedure (i) to (iv) can be used for any choice of polar axis. It will for instance supply three independent tests if one chooses

transversity, $s$-helicity, or $t$-helicity quantization axes. Furthermore, if one measures all the multipoles $y_M^{(L)}$ for any system of quantization axes, one can transform these measurements by convenient rotations and apply the procedure (i) - (iv) to all possible choices of polar axis.

4.2.1. Decay mode (1): $j \to 0 + 0$.

*Case* (a) The intersection of the simplices $\lambda_1 \mathcal{D}_j^{(D,E)}$ by the two-plane $\{\lambda_1^2\eta^2, \lambda_1^4\eta^4\}$ are shown in fig. 10 (a) for $j = 1, 2, 3, 4, \infty$ and are respectively labelled by the letters $A$, $bB$, $c$, $d$ and $z$. Note that the segment $A_0A_1$ and the isosceles triangle $B_0B_1B_2$ represent the whole domains $\lambda_1 \mathcal{D}_1^{(D,E)}$ and $\lambda_1 \mathcal{D}_2^{(D,E)}$ respectively.

If the experimental point $\hat{y}$ falls near $A_0$ the spin must be $j = 1$, and if it falls near $B_0$ or $B_1$, it must be $j = 2$. There are also small regions which establish $j \leq 3$, $j \leq 4 \ldots$ On the other hand it is difficult to give a lower limit for the spin. And if $\hat{y}$ falls near $A_1$, the tests is completely powerless. Indeed the polygon sides $b_0$, $c_0$, $d_0, \ldots z_0$ lie all in the same straight line, the common boundary imposed by the positivity of the central density matrix element $\rho_{00} \geq 0$. Note that a violation of this boundary comes from an angular distribution which is negative for some value of $\theta$, since $\overline{B_1B_2}$ is also boundary of the dotted "parachute-shaped" domain.

*Case* (b) Part (b) of the fig. 10 shows the corresponding projections of the same simplices $\lambda_1 \mathcal{D}_j^{(D,E)}$. Note that there are still regions which can establish $j = 1$ (near $A_0$), $j = 2$ (near $B_0$ or $B_1$) and even $j = 3$ (near $C_2$). It is interesting that if $\hat{y}$ falls in the neighborhood of $B_2$, $C_3, D_4 \ldots Z_\infty$ a lower limit for $j$ can be established.

In the case of collinear production in a reaction of the type (91), and for helicity quantization, the allowed regions for $\hat{y}$ are the segments $\overline{A_0A_1}$ $\overline{B_0B_1}$, $\overline{C_0C_1}$, $\overline{D_0D_1}, \ldots Z_0$. This could fix an upper limit to the spin.

4.2.2. Decay mode (1'): $j^\eta \to j^{\eta_1} + 0^{\eta_0}$ with $\eta\eta_1\eta_0 = (-1)^j$.

*Case* (a) The intersections of the simplices $\lambda_1, \mathcal{D}_j^{(D,E)}$ shown in fig. 11 (a) are smaller than those in fig. 10 (a), and therefore they supply in general weaker spin tests. Nevertheless it is interesting that some negative value of $\lambda_1^4, \eta^4$ establishes $j = 2$, and that some big absolute value of the same $\lambda_1^4, \eta^4$ excludes $j = 3$. Note that now it is the boundary given by $\rho_{11} \geq 0$ which lies in the same straight line for the different spin values. But the corresponding domains do not superpose each other on this line.

*Case* (b) The projection of the simplices $\lambda_1, \mathcal{D}_j^{(D,E)}$ are shown in fig. 11 (b). There is still near $B_0$ a region which could establish $j = 2$, and large regions which could give lower limits for $j$.

In the case of collinear reaction of type (91) the allowed regions $\overline{A_0A_1}$,

$\overline{B_0B_1}$, $\overline{C_0C_1}$, $\overline{D_0D_1}$, ... $Z_0$ are more clearly distinguished than in fig. 10 (b).

4.2.3. Decay mode (2): $j \to \frac{1}{2} + 0$.

*Case* (a) The intersections of the simplices $\lambda_2 \mathcal{D}_j^{(D,E)}$ shown in fig. 12 (a) are in some way similar to those shown in fig. 10 (a) for spin half-a-unit greater. They present the same common boundary and no test is possible near $A_3$.

*Case* (b) The projections of $\lambda_2 \mathcal{D}_j^{(D,E)}$ shown in fig. 12 (b) can supply a lower limit for $j$.

In the case of collinear reaction of type (92) and helicity quantization, only the points $A_1$, $B_1$, $C_1 \ldots Z_1$ are allowed. The historical test proposed by Adair [10], has yielded spin $j = \frac{1}{2}$ for $\Lambda^0$ by a polarization point $\hat{y}$ near the point $O$, clearly separated from $A_1 \ldots Z_1$. Note that for higher spin this test is not so clear cut.

Table 5 gives the coordinates and equations for all the figures of sect. 4.

The first expression in its part (a) can be used for studying higher projections of the simplices $\lambda_i \mathcal{D}_j^{(D)}$, since it gives all the coordinates for their vertices.

## 5. CONCLUSION

We have studied separately each of the three decay modes (i). However one should never forget that a particle can have competing decay modes of different types. Their simultaneous observation may lead to powerful spin tests. Consider, for instance, a meson resonance with the two competing decay modes (1) and (1'). The $y_M^{(L)}$ coefficients of the two angular distributions of the decay products from the same decaying state are proportional (see subsect. 2.2.2 and table 1). Indeed:

$$\frac{y_M^{(L)}(1')}{y_M^{(L)}(1)} = \frac{\lambda_{1'}(L, j)}{\lambda_1(L, j)} = -(2j+1) \begin{Bmatrix} j & j & L \\ j & j & 1 \end{Bmatrix} = 1 - \frac{L(L+1)}{2j(j+1)}. \tag{95}$$

As far as we know this formula was first obtained by de Rafael [11], who proposed this test for the $A_2$ meson.

As a general rule, the more an angular distribution is isotropic, the less it is expected to be useful for spin determination. However a quite anisotropic angular distribution may also be disappointing, from the point of view of spin test, as some of our figures show.

Since most of the new resonances are not very sharply defined, we are aware of the difficulties which arise for the interpretation of experimental results. It is however astonishing that *all* the consequences of angular

momentum and parity conservation are not generally used in the exploitation of the data. For example, if there are non vanishing $y_M^L$ in the angular distribution of a decay of type (i), only up to $L = L_0$ ‡, every one knows that the spin $j$ of the decaying particle satisfies $j \geq \frac{1}{2} L_0$. But one can say more, and our paper gives the relevant criteria for establishing the possible value of $j$.

We have applied for ourselves the methods of this paper to analyze some published data, but we feel that such an analysis cannot be keenly performed without the collaboration of the experimental authors.

Each author is grateful to the other two's institutions, for making the meetings possible. P. Minnaert thanks also the French "Commission des Grands Accélérateurs". M. G. Doncel benefited by an invitation to the IHES, and acknowledges the partial support of the Spanish "Grupo Interuniversitario de Física Teórica". The authors also thank Hewlett-Packard, France, and its director P. Ardichvili, for their help with the desk calculator and plotter used for the figures.

## APPENDIX

A.1. *Invariance of $\partial \mathcal{D}_j$ by polar transformation*

In the space $\mathcal{E}_{N+1}$, with origin $O$ and scalar product (5), consider the cone $\mathcal{C}$ of non negative matrices, with vertex at $O$. We remark that if $O \neq \rho_1, \rho_2 \in \mathcal{C}$, then $\mathrm{tr}\, \rho_1 \rho_2 \geq 0$. The equality appears if and only if both $\rho_1$ and $\rho_2$ have ranks strictly smaller than $2j+1$, i.e. $\rho_1, \rho_2$ belong to $\partial \mathcal{C}$, the boundary of $\mathcal{C}$, and furthermore $\rho_1 \rho_2 = \rho_2 \rho_1 = 0$. (Cf. e.g. ref. [1, 2].) To summarize, the conditions

$$O \neq \rho_1, \rho_2 \in \mathcal{C}\ , \qquad \mathrm{tr}\, \rho_1 \rho_2 = 0\ , \tag{A(1)}$$

imply

$$\rho_1, \rho_2 \in \partial \mathcal{C}\ , \quad \rho_1 \rho_2 = \rho_2 \rho_1 = 0\ , \quad \mathrm{rank}\, \rho_1 + \mathrm{rank}\, \rho_2 \leq 2j+1\ . \tag{A(2)}$$

We shall use a more geometrical approach. Let us denote by $T_\rho$ the hyperplane through $O$ perpendicular to the straight line $\overline{\rho O}$. If $\rho_1 \in \partial \mathcal{C}$, then it has one or several zero eigenvalues and the Hermitean projectors on the corresponding eigenstates belong to $T_{\rho_1} \cap \mathcal{C}$. Moreover all vectors of this intersection, like $\rho_2$, satisfy eq. A(1) and therefore eq. A(2). In the language of complex projective geometry, $\partial \mathcal{C}$ is self conjugated with respect to $S$, the null radius sphere centered at $O$; moreover conjugated

‡ As a matter of fact, the $|y_M^{(L)}|$ often decrease with $L$ while the errors on $|y_M^{(L)}|$ increase with $L$. So for $L > L_0$, it would be more rigorous to say that the values of the $y_M^{(L)}$ are *compatible* with zero.

points of $\mathcal{C}$ have the property A(2). Therfore, if $H$ is any hyperplane of $\mathcal{E}_{N+1}$, cutting $\mathcal{C}$, the intersection $H \cap \partial\mathcal{C}$ is self transformed by the polar transformation with respect to the imaginary sphere $S_H = H \cap S$. In particular, for the hyperplane $\mathcal{E}_N$ whose distance from $O$ is

$$|O\rho_0| = [\mathrm{tr}\,\rho_0^2]^{\frac{1}{2}} = [2j+1]^{-\frac{1}{2}}, \qquad \text{A(3)}$$

the corresponding sphere, $S_N \cap \mathcal{E}_N$ is the imaginary sphere of center $\rho_0$ and radius $[-1/(2j+1)]^{\frac{1}{2}}$. With the renormalization of the metric defined by equation (9) this radius becomes $[-1/2j]^{\frac{1}{2}}$. Since we have $\partial\mathcal{D}_j = \partial\mathcal{C} \cap \mathcal{E}_N$, we have proven:

*Theorem* 1. The boundary $\partial\mathcal{D}_j$ is invariant by the polar tranformation with respect to the imaginary sphere $S_N$ of center $\rho_0$ and radius $[-1/2j]^{\frac{1}{2}}$. Moreover if $\rho_1, \rho_2 \in \partial\mathcal{D}_j$ are conjugated with respect to $S_N$, they satisfy: $\mathrm{rank}\,\rho_1 + \mathrm{rank}\,\rho_2 \leq 2j+1$.

We remind the reader that this polar transformation is also the product of the polar transformation with respect to the real sphere of center $\rho_0$ and radius $[1/2j]^{\frac{1}{2}}$, and the reflection through the point $\rho_0$.

Let $P_i$ the orthogonal projector in $\mathcal{E}_N$ on the $k$-plane $P_i\,\mathcal{E}_N$ which contains $\rho_0$. From theorem 1, by elementary geometrical arguments, we deduce:

*Corollary* 1. The intersection $\partial\mathcal{D}_i \cap P_i\,\mathcal{E}_N = \partial(\mathcal{D}_j \cap P_i\,\mathcal{E}_N)$ and the projection $P_i\,\partial\mathcal{D}_j = \partial P_i\,\mathcal{D}_j$ are polar transform of each other with respect to the spheres $S_N \cap P_i\,\mathcal{E}_N$.

We will give a second proof of this theorem and its corollary, in order that they become more intuitive to readers untrained in complex projective geometry.

As we have seen the $(2j+1)$ by $(2j+1)$, trace one, Hermitean matrices $R$ form a Euclidean space $\mathcal{E}_N$ $(N = (2j+1)^2 - 1)$ and this space can be spanned by an orthogonal basis formed by the matrices $Q(j)_M^{(L)}$, $1 \leq L \leq 2j$, $-L \leq M \leq L$, introduced in the eqs. (43). These matrices satisfy:

$$Q(j)_M^{(L)} = Q(j)_M^{(L)*}, \qquad \mathrm{tr}\,Q(j)_M^{(L)} = 0, \qquad \text{A(4)}$$

$$Q(j)_M^{(L)} = \overline{Q(j)_M^{(L)}} = Q(j)_M^{(L)T} \quad \text{for} \quad M \geq 0, \qquad \text{A(5a)}$$

$$Q(j)_M^{(L)} = \overline{-Q(j)_M^{(L)}} = -Q(j)_M^{(L)T} \quad \text{for} \quad M < 0, \qquad \text{A(5b)}$$

$$\mathrm{tr}\,Q(j)_M^{(L)} Q(j)_{M'}^{(L')} = \frac{2j+1}{2j}\,\delta_{LL'}\,\delta_{MM'}. \qquad \text{A(6)}$$

The expansion of $R \in \mathcal{E}_N$ on this basis is:

$$R = \frac{1}{2j+1}\left(\mathbb{1} + 2j \sum_{L=1}^{2j} \sum_{M=-L}^{+L} r_M^{(L)}\, Q(j)_M^{(L)}\right), \qquad \text{A(7)}$$

and its coordinates are the scalar products

$$r_M^{(L)} = (\rho, Q(j)_M^{(L)}) \equiv \mathrm{tr}\,\rho\, Q(j)_M^{(L)} . \qquad \text{A(8)}$$

Since the matrices $Q(j)_M^{(L)}$ are Hermitean, their eigenvalues are real. We note $\mu(j, L, M)$ the largest eigenvalue of $Q(j)_M^{(L)}$ and $-\nu(j, L, M)$ its smallest one. From eqs. A(4) and A(6) we deduce the relations

$$-1 \leqslant -\nu(j, L, M) < 0 < \mu(j, L, M) \leqslant 1 , \qquad \text{A(9)}$$

where the equalities hold for $j = \frac{1}{2}$ only.

Let $\boldsymbol{u}$ be a unit vector of $\mathcal{E}_N$ and $u_M^{(L)}$ its real coordinates:

$$\boldsymbol{u}^2 \equiv \sum_{L=1}^{2j} \sum_{M=-L}^{+L} u_M^{(L)2} = 1 . \qquad \text{A(10)}$$

With this vector one can build the matrix

$$Q(j, \boldsymbol{u}) = \sum_{L=1}^{2j} \sum_{M=-L}^{+L} u_M^{(L)} Q(j)_M^{(L)} . \qquad \text{A(11)}$$

Using eqs. A(4) and A(6) one shows that $Q(j, \boldsymbol{u})$ has the properties:

$$Q(j, \boldsymbol{u})^* = Q(j, \boldsymbol{u}) , \qquad \mathrm{tr}\, Q(j, \boldsymbol{u}) = 0 , \qquad \text{A(12)}$$

$$\mathrm{tr}\, Q(j, \boldsymbol{u})\, Q(j, \boldsymbol{u}') = \frac{2j+1}{2j} \sum_{L, M} u_M^{(L)} u'^{(L)}_M , \qquad \text{A(13)}$$

and one deduces that the largest and smallest eigenvalues of $Q(j, \boldsymbol{u})$, noted $\mu(j, \boldsymbol{u})$ and $-\nu(j, \boldsymbol{u})$ satisfy the inequalities

$$-1 \leqslant -\nu(j, \boldsymbol{u}) < 0 < \mu(j, \boldsymbol{u}) \leqslant 1 . \qquad \text{A(14)}$$

Note that

$$Q(j, -\boldsymbol{u}) = -Q(j, \boldsymbol{u}) , \qquad \text{A(15)}$$

and thus

$$\nu(j, -\boldsymbol{u}) = \mu(j, \boldsymbol{u}) . \qquad \text{A(16)}$$

Let us consider the trace one, Hermitean matrices $R(\boldsymbol{u}, \lambda)$ defined by

$$R(\boldsymbol{u}, \lambda) = \frac{1}{2j+1} (\mathbb{1} + 2j\lambda Q(j, \boldsymbol{u})) , \qquad \lambda \text{ real} . \qquad \text{A(17)}$$

(i) The one dimensional subspace of $\mathcal{E}_N$ generated by $\boldsymbol{u}$ is the set

$$\{R(\boldsymbol{u})\} = \{R(\boldsymbol{u}, \lambda) \mid -\infty \leqslant \lambda \leqslant \infty\} . \qquad \text{A(18)}$$

(ii) The intersection $\{\rho(\boldsymbol{u})\} = \mathcal{D}_j \cap \{R(\boldsymbol{u})\}$ of the positivity domain $\mathcal{D}_j$ with this one dimensional subspace is the subset of non negative matrices:

$$\{\rho(\boldsymbol{u})\} = \{R(\boldsymbol{u}, \lambda) \mid -b(\boldsymbol{u}) \leq \lambda \leq a(\boldsymbol{u})\} , \qquad \text{A(19)}$$

where the extremal values, deduced from the positivity of the eigenvalues of $R(\boldsymbol{u}, \lambda)$ are

$$-b(\boldsymbol{u}) = \frac{-1}{2j\,\mu(j, \boldsymbol{u})}, \qquad a(\boldsymbol{u}) = \frac{1}{2j\,\mu(j, -\boldsymbol{u})}. \qquad \text{A(20)}$$

(iii) The projection $\{P_{\boldsymbol{u}}\,\mathcal{D}_j\}$ of the positivity domain $\mathcal{D}_j$ on the one dimensional subspace $\{R(\boldsymbol{u})\}$ is the subset

$$\{P_{\boldsymbol{u}}\,\mathcal{D}_j\} = \{R(\boldsymbol{u}, \lambda) \mid -\tilde{b}(\boldsymbol{u}) \leq \lambda \leq \tilde{a}(\boldsymbol{u})\} , \qquad \text{A(21)}$$

where the extremal values are, according to eq. A(8),

$$-\tilde{b}(\boldsymbol{u}) = \operatorname*{Min}_{\rho \in \mathcal{D}_j} \operatorname{tr} \rho Q(j, \boldsymbol{u}) , \qquad \tilde{a}(\boldsymbol{u}) = \operatorname*{Max}_{\rho \in \mathcal{D}_j} \operatorname{tr} \rho Q(j, \boldsymbol{u}) . \qquad \text{A(22)}$$

These extremal values are reached when $\rho$ is chosen as the rank one projector of the eigenvector of $Q(j, \boldsymbol{u})$, for its smallest and largest eigenvalues, so

$$-\tilde{b}(\boldsymbol{u}) = -\mu(j, -\boldsymbol{u}) , \qquad \tilde{a}(\boldsymbol{u}) = \mu(j, \boldsymbol{u}) . \qquad \text{A(23)}$$

We remark that

$$\frac{\tilde{a}(\boldsymbol{u})}{a(\boldsymbol{u})} = \frac{\tilde{b}(\boldsymbol{u})}{b(\boldsymbol{u})} = 2j\,\mu(j, \boldsymbol{u})\,\mu(j, -\boldsymbol{u}) > 0 , \qquad \text{A(24)}$$

$$-b(\boldsymbol{u})\tilde{a}(\boldsymbol{u}) = -\tilde{b}(\boldsymbol{u})a(\boldsymbol{u}) = \frac{-1}{2j} . \qquad \text{A(25)}$$

The boundary $\partial\,\mathcal{D}_j$ of $\mathcal{D}_j$ is the set of points $\{\boldsymbol{u}\,a(\boldsymbol{u})\}$ for all unit vectors $\boldsymbol{u}$. The convexity of $\mathcal{D}_j$ implies that for each unit vector $\boldsymbol{u}$, there are at most two hyperplanes perpendicular to $\boldsymbol{u}$ and tangent to $\mathcal{D}_j$. The points $\boldsymbol{u}\tilde{a}(\boldsymbol{u})$ and $-\boldsymbol{u}\tilde{b}(\boldsymbol{u}) = -\boldsymbol{u}\tilde{a}(-\boldsymbol{u})$ are the feet of the perpendiculars from $\rho_0$ to these two tangent planes. The set of points $\{\boldsymbol{u}\tilde{a}(\boldsymbol{u})\}$ is called the pedal surface ‡ of $\partial\mathcal{D}_j$. Eq. A(25) shows that $\partial\mathcal{D}_j$ and its pedal surface are transformed of each other by the inversion in the sphere $S_N$ of center $\rho_0$ and imaginary radius $[-1/2j]^{\frac{1}{2}}$. Since the inverse in $S_N$ of the pedal surface of any surface $\Sigma$ is the polar transform of $\Sigma$ with respect to $S_N$, this proves the first property of theorem 1.

Let $\boldsymbol{u}'a(\boldsymbol{u}')$ be a point of $\partial\mathcal{D}_j$ conjugated of $\boldsymbol{u}\,a(\boldsymbol{u})$ i.e. $\boldsymbol{u}\cdot\boldsymbol{u}'a(\boldsymbol{u})\,a(\boldsymbol{u}') = -1/2j$. This imposes that the matrices $\rho'$ and $\rho$ represented by these points (cf. eq. (9)) satisfy

$$\frac{2j+1}{2j} \operatorname{tr}(\rho - \rho_0)(\rho' - \rho_0) = -\frac{1}{2j} ,$$

which is equivalent to $\operatorname{tr}\rho\rho' = 0$. This ends the second proof of theorem 1. Let $P_i$ be the orthogonal projector in $\mathcal{E}_N$ on $\mathcal{E}_i = P_i\,\mathcal{E}_N$, a $k$-plane which

‡ In French, "la podaire".

contains $\rho_0$. Our second proof shows explicitly that the intersection $\mathcal{E}_i \partial \mathcal{D}_j$ is the inverse in $S_i = S_N \mathcal{E}_i$ of the pedal curve of the projection $P_i \partial \mathcal{D}_j = \partial P_i \mathcal{D}_j$, so for any $k$-plane $\Sigma_i$, intersection and projection of $\partial \mathcal{D}_j$ are polar transforms of each other with respect to $S_i$.

We now study some special properties of the directions of the orthonormal basis of the $Q^{(L)}_M$. When $\boldsymbol{u}$ has only one non vanishing component, $u^{(L)}_M = 1$, we denote the $a(\boldsymbol{u})$, $\tilde{a}(\boldsymbol{u})$, $b(\boldsymbol{u})$, $\tilde{b}(\boldsymbol{u})$ by $a^{(L)}_M$, $\tilde{a}^{(L)}_M$, $b^{(L)}_M$, $\tilde{b}^{(L)}_M$.

Eq. (38) shows that a rotation around the quantization axis, by an angle $\epsilon\pi/4M$, $\epsilon^2 = 1$, multiplies $T(j)^{(L)}_M$ by $\epsilon i$, and eq. (43) shows that the $Q(j)^{(L)}_M$ are transformed according to the law:

$$M \neq 0\ ,\quad Q(j)^{(L)}_M \to -\epsilon(\text{sign of } M)\, Q(j)^{(L)}_{-M}\ . \qquad \text{A(26)}$$

This shows, for $M \neq 0$, that $Q(j)^{(L)}_M$, $Q(j)^{(L)}_{-M}$, $-Q(j)^{(L)}_{-M}$ are conjugated by $D^{(j)}(n_3, \pi/4M)$; hence they have same eigenvalues and their set of eigenvalues is invariant by multiplication by -1. In particular for

$$M \neq 0\ ,\quad \nu(j, L, M) = \nu(j, L, -M) = \mu(j, L, M) = \mu(j, L, -M) \qquad \text{A(27)}$$

and from eqs. A(20) and A(23)‡ for

$$M \neq 0\ ,\quad b^{(L)}_{-M} = b^{(L)}_M = a^{(L)}_M = a^{(L)}_{-M}\ ;\ \tilde{b}^{(L)}_{-M} = \tilde{b}^{(L)}_M = \tilde{a}^{(L)}_M = \tilde{a}^{(L)}_{-M}\ . \qquad \text{A(28)}$$

The rotation of $-\pi$ around the second axis is represented by

$$D^{(j)}(n_2, -\pi)^M_{M'} = \Gamma(j)^M_{M'} = (-1)^{j-M} \delta_{M,-M'}\ . \qquad \text{A(29)}$$

It transforms $Q(j)^{(L)}_M$ into $(-1)^L Q(j)^{(L)}_M$. So the equalities A(27) and A(28) can be extended to the case $M = 0$ for odd $L$.

A.2. *Invariance of $\partial\Delta$ by polar transformation*

We consider the real measures on the unit sphere $\Omega$ of the three-dimensional space. The measures which satisfy

$$\int f \mathrm{d}\Omega = 1 \qquad \text{A(30)}$$

form a vector space $\mathcal{M} \supset \mathcal{Y}$, with the same origin $\mathcal{I}_0$ as $\mathcal{Y}$ (cf. eq. (27)). The non-negative measures of $\mathcal{M}$ form a convex domain $\Delta^-$, the closure of $\Delta$. The extremal points of $\Delta^-$ are the Dirac measures $\delta_\omega$, $\omega \in \Omega$.

Let $v$ be a real, norm one, bounded function of the Hilbert space $\mathcal{Y}'$ (cf. eq. (26)):

$$(v, v) = \int v^2 \mathrm{d}\Omega = 1\ , \qquad \text{A(31)}$$

‡ In ref. [12] the second part of eq. A(28) is proven and numerical values of $\tilde{a}^{(L)}_M$ are given for $j \leq 2$.

$$-\nu(v) = \underset{\omega \in \Omega}{\text{Min}}\ v(\omega) = v(\omega_m) \text{ finite} , \qquad \text{A(32a)}$$

$$\mu(v) = \underset{\omega \in \Omega}{\text{Max}}\ v(\omega) = v(\omega_M) \text{ finite} , \qquad \text{A(32b)}$$

such that

$$\frac{1}{4\pi} + v \in \mathcal{V} \ , \quad \text{i.e.} \int v \, d\Omega = 0 . \qquad \text{A(33)}$$

From eqs. A(32) and A(33) one deduces:

$$-\nu(v) \leq 0 \leq \mu(v) , \qquad \text{A(34)}$$

$$\nu(-v) = \mu(v) . \qquad \text{A(35)}$$

Let us consider the functions $F(v, \lambda) \in \mathcal{V} \subset \mathcal{M}$ defined by

$$F(v, \lambda) = \frac{1}{4\pi} + \lambda v , \qquad \lambda \text{ real} . \qquad \text{A(36)}$$

(i) The one dimensional subspace of $\mathcal{V}$ generated by $v$ is the set

$$\{F(v)\} = \{F(v, \lambda) \mid -\infty \leq \lambda \leq \infty\} . \qquad \text{A(37)}$$

(ii) The intersection $\{\mathcal{I}(v)\} = \Delta \cap \{F(v)\}$ of the angular distribution domain $\Delta$ with this one dimensional subspace is

$$\{\mathcal{I}(v)\} = \{F(v, \lambda) \mid -b(v) \leq \lambda \leq a(v)\} , \qquad \text{A(38)}$$

where the extremal values, deduced from the positivity of $\mathcal{I}(v)$ are

$$b(v) = \frac{1}{4\pi\mu(v)}, \qquad a(v) = \frac{1}{4\pi\nu(v)} . \qquad \text{A(39)}$$

(iii) Let $P_v$ be the projector on the one dimensional subspace $\{F(v)\}$ of $\mathcal{M}$:

$$P_v f = v(v, f) = v \int v f \, d\Omega . \qquad \text{A(40)}$$

The projection $\{P_v \Delta^-\}$ of the closure of the angular distribution domain on the one dimensional subspace $\{F(v)\}$ is

$$\{P_v \Delta^-\} = \{F(v, \lambda) \mid -\tilde{b}(v) \leq \lambda \leq \tilde{a}(v)\} , \qquad \text{A(41)}$$

with

$$-\tilde{b}(v) = \underset{f \in \Delta^-}{\text{Min}}\ (v, f) = \int v \delta_{\omega_m} \, d\Omega = v(\omega_m) = -\nu(v) , \qquad \text{A(42a)}$$

$$\tilde{a}(v) = \underset{f \in \Delta^-}{\text{Max}}\ (v, f) = \int v \delta_{\omega_M} \, d\Omega = v(\omega_M) = \mu(v) . \qquad \text{A(42b)}$$

Note that $P_v \Delta^-$ is the closure of $P_v \Delta$.

From eqs. A(35) and A(42) one deduces:

$$\tilde{a}(-v) = \tilde{b}(v) , \qquad \text{A(43)}$$

$$\frac{\tilde{a}(v)}{a(v)} = \frac{\tilde{b}(v)}{b(v)} = 4\pi\mu(v)\nu(v) > 0 , \qquad \text{A(44)}$$

$$-b(v)\tilde{a}(v) = -\tilde{b}(v)a(v) = -\frac{1}{4\pi} . \qquad \text{A(45)}$$

So, for any finite dimensional space $\mathcal{Y}_i = P_i\,\mathcal{Y} \subset \mathcal{Y}$, we conclude that $\Delta \cap \mathcal{Y}_i$ and $P_i\Delta$ are polar transforms of each other with respect to the sphere of radius $R = \sqrt{-1/4\pi}$, centered at the origin $\mathcal{Y}_0 = 1/4\pi$ of $\mathcal{Y}$.

A.3. *Dipole intersection* $\mathcal{D}_j^{(1)}$ *and projection* $\tilde{\mathcal{D}}_j^{(1)}$

For $L = 1$, the $Q(j)_M^{(1)}$ are three orthogonal components of the dipole and they can be transformed into each other by "rotations" (cf. eqs. (38) and (43)). From this remark and from the general expression of the matrix elements of $Q(j)_M^{(1)}$ (cf. eqs. (37) and (43)) we deduce that

$$\nu(j, 1, M) = \mu(j, 1, M) = \sqrt{\frac{3}{2j+2}} , \qquad \text{A(46)}$$

which is independent of $M$. So $\mathcal{D}_j^{(1)}$ and $\tilde{\mathcal{D}}_j^{(1)}$ are two spheres in the three-dimensional space $\mathcal{E}^{(1)}$ of radius respectively equal to (cf. eqs. A(20) and A(23))

$$r^{(1)} = \frac{1}{j}\sqrt{\frac{j+1}{6}} , \qquad \text{A(47a)}$$

$$\tilde{r}^{(1)} = \sqrt{\frac{3}{2j+2}} . \qquad \text{A(47b)}$$

Note that

$$\tilde{r}^{(1)}/r^{(1)} = 3j/(j+1) , \qquad \tilde{r}^{(1)}r^{(1)} = \frac{1}{2j} , \qquad \text{A(47c)}$$

which are eqs. A(24), A(25) for the dipole.

Consider the decay $j \to \frac{1}{2} + 0$. The coefficient $\lambda(1, j)$ of this decay is different from zero only if parity is violated; then it is dynamic dependent, but it is still given, for $L = 1$, by table 1 (c), up to a factor $\chi$, $-1 \leq \chi \leq 1$, instead of $\frac{1}{2}(1 + (-1)^L)$. The coefficient $\chi$ contains the dependence on the parity violating dynamics; it is the asymmetry parameter. Hence the observed $y_M^{(1)}$ are related to the normalized $r_M^{(1)}$ by:

$$y_0^{(1)} = \chi(-1)^{j-\frac{1}{2}}\sqrt{2j(2j+1)}\begin{pmatrix} 1 & j & j \\ 0 & \frac{1}{2} & -\frac{1}{2} \end{pmatrix} r_M^{(1)} = \chi\frac{1}{\sqrt{2j+2}} r_0^{(1)} , \qquad \text{A(48a)}$$

$$-\sqrt{2}\,\mathrm{Re}\,y_1^{(1)} = \chi\frac{1}{\sqrt{2j+2}}r_1^{(1)}\,, \qquad -\sqrt{2}\,\mathrm{Im}\,y_1^{(1)} = \chi\frac{1}{\sqrt{2j+2}}r_{-1}^{(1)}\,. \tag{A(48b)}$$

From eq. A(47b), conservation of angular momentum implies, for the invariant

$$\sum_{M=-1}^{1} |y_M^{(1)}|^2$$

that one can extract from the data, the condition

$$\left[\sum_{M=-1}^{1} |y_M^{(1)}|^2\right]^{\frac{1}{2}} \leq |\chi|\frac{\tilde{r}^{(1)}}{\sqrt{2j+2}} = |\chi|\frac{\sqrt{3}}{2j+2} \leq \frac{\sqrt{3}}{2(j+1)}. \tag{A(49a)}$$

Moreover, if the only non vanishing $y_M^{(L)}$ are those for $L = 1$, we have the stronger (when $j \leq \frac{1}{2}$) condition

$$\left[\sum_{M=-1}^{1} |y_M^{(1)}|^2\right]^{\frac{1}{2}} \leq |\chi|\frac{r^{(1)}}{\sqrt{2j+2}} = |\chi|\frac{1}{2\sqrt{3j}} \leq \frac{1}{2\sqrt{3j}}. \tag{A(49b)}$$

This is the test proposed by Lee and Yang [13] for the $\Lambda^0$ decay. One can always choose the quantization axis such that $y_{\pm 1}^{(1)} = 0$; instead of the expectation value of $\sqrt{4\pi}\langle Y_0^{(1)}\rangle = \langle\sqrt{3}\cos\theta\rangle$, Lee and Yang studied $\langle\cos\theta\rangle$ so their limits are $1/\sqrt{3}$ those of the eqs. A(49).

We have studied the well-known case $L = 1$ in order to help the understanding of the case $L = 2$.

A.4. *The quadrupole space*

We have to study the action of the "rotation" group SO(3) on $\mathcal{E}^{(2)}$, the five dimensional real space of the irreducible representation $D^{(2)}$. In order to study this action we can use any one of the equivalent realizations of this representation. An elegant realization of $\mathcal{E}^{(2)}$ (used in the theory of quadrics) is to consider it as the space of the $3 \times 3$, traceless, real, symmetrical matrices:

$$\mathrm{tr}\,x = 0\,, \qquad \bar{x} = x\,, \qquad x^{\mathrm{T}} = x\,. \tag{A(50)}$$

The group SO(3), i.e. the group of $3 \times 3$ matrices which satisfy

$$\bar{a} = a\,, \qquad a^{\mathrm{T}} = a^{-1}\,, \qquad \det a = 1\,, \tag{A(50')}$$

acts on this realization $\mathcal{E}^{(2)}$ according to

$$D(a)x = a\,x\,a^{\mathrm{T}} = a\,x\,a^{-1}\,. \tag{A(51)}$$

This action is orthogonal, and leaves invariant on $\mathcal{E}^{(2)}$ the Euclidian scalar product

$$(x, y) = \operatorname{tr} xy \ . \qquad \text{A(52)}$$

As is well known, by the transformation A(51) of an orthogonal matrix $a$, any $x$ can be diagonalized and its eigenvalues put in a decreasing order $\xi_1 \geqslant \xi_2 \geqslant \xi_3$, $\xi_1 + \xi_2 + \xi_3 = 0$. We can also say equivalently that the coefficients of the characteristic equation of $x$

$$x^3 - \tfrac{3}{4}\alpha(x)\, x + \tfrac{1}{4}\beta(x)\, I = 0 \ , \qquad \text{A(53)}$$

with

$$\alpha(x) = \tfrac{2}{3}(x, x) = \tfrac{2}{3} \operatorname{tr} x^2 \ , \qquad \text{A(54a)}$$

$$\beta(x) = -4 \det x \ , \qquad \text{A(54b)}$$

characterize completely the orbits of SO(3) on $\mathcal{E}^{(2)}$, i.e., $x$ and $x'$ can be transformed into each other by SO(3) transformation if and only if $\alpha(x) = \alpha(x')$ and $\beta(x) = \beta(x')$. Since $x$ is Hermitean, it must have three real eigenvalues so

$$4\,(\tfrac{3}{4}\alpha(x))^3 \geqslant 27\,(\tfrac{1}{4}\beta(x))^2 \ , \qquad \text{A(55)}$$

i.e.

$$-\alpha(x)^{\frac{3}{2}} \leqslant \beta(x) \leqslant \alpha(x)^{\frac{3}{2}} \ . \qquad \text{A(55')}$$

We are interested by the realization of $\mathcal{E}^{(2)}$ as the five dimensional real vector space of Hermitean traceless matrices

$$\rho'(j) = \frac{2j+1}{2j}\rho(j)^{(2)} = \sum_{M=-2}^{2} r_M^{(2)} Q(j)_M^{(2)} = \frac{\sqrt{5\,(2j+1)}}{2j} \sum_{M=-2}^{2} \overline{t_M^{(2)}}\, T(j)_M^{(2)} \ . \qquad \text{A(56)}$$

This realization is $j$ dependent, but eq. (38) shows that the action of SO(3) on these quadrupole spaces is $j$-independent. Indeed for the "rotation" $R$

$$T(j)_M^{(2)} \rightsquigarrow T(j)_{M'}^{(2)} D^{(2)}(R)_M^{M'} \ . \qquad \text{A(57)}$$

We therefore consider the quadrupole space $j = 1$. The $\rho'(1)$ are $3 \times 3$ traceless matrices and one passes from the $x$ to the $\rho'(1)$ by a change of basis in the three dimensional space; i.e. the sets of $x'(1)$ and of $x = x^{\mathrm{T}}$ are conjugated by a fixed matrix. This conjugation does not change the trace (= 0), the trace of the square, or the determinant. Hence $\alpha[\rho'(1)]$ and $\beta[\rho'(1)]$ characterize the orbits of SO(3) for this realization of $\mathcal{E}^{(2)}$. The expressions (54) of $\alpha$ and $\beta$ as function of $r_M^{(L)}$ can therefore be computed from eqs. A(54) with

$$x = \sum_{M=-2}^{2} r_M^{(2)} Q(1)_M^{(2)} \ . \qquad \text{A(58)}$$

The $Q(1)_M^{(2)}$ are defined by eqs. (43) and (37). They are explicitly given in ref. [1], IA2 table 1, ref. [2], I2 table 1.

Remark that the four $Q(j)^{(2)}_{M}$, $M \neq 0$ are on the same orbit $\alpha = 1$, $\beta = 0$, but $Q(j)^{(2)}_{0}$ is in a different orbit $\alpha = 1$, $\beta = 1$.

## REFERENCES


[1] M. G. Doncel, L. Michel and P. Minnaert, Polarization density matrix, issues 1, 2, 3 (preprints of the Laboratoire de Physique Théorique, Université de Bordeaux: PTB 35, 37, 41).
[2] M. G. Doncel, L. Michel and P. Minnaert, Matrices densité de polarisation, summer school of Gif-sur-Yvette 1970, (Ed. R. Salmeron, Laboratoire de Physique de l'Ecole Polytechnique, Paris).
[3] W. F. Cartwright, C. Richman, M. N. Whitehead and H. A. Wikon, Phys. Rev. 91 (1953) 677.
[4] L. Michel, Nuovo Cimento 10 (1953) 319; and Comptes Rendus Conf. Bagnères, p. J.3 (Ed., Ecole Polytechnique, Paris, 1953).
[5] F. F. Christy and S. Kusaka, Phys. Rev. 59 (1941) 414.
[6] A. Eskreys, P. Malechi, K. Zalewski, A. Białas, A. Kotański, B. Muryn, E. de Wolf, F. Grard, F. Verbeure, R. Windmolders, Y. Goldschmidt-Clermont, A. Grant, V. P. Henri, B. Jongejans and H. Piotrowska, Nucl. Phys. B29 (1971) 587.
[7] Å. Bohr, Nucl. Phys. 10 (1959) 486.
[8] E. de Rafael, Théorie relativiste des corrélations angulaires et application à l'analyse phénoménologique des particules et résonances, Ann. Inst. Henri Poincaré, V2, 83-204 (1966).
[9] J. T. Donohue and H. Högaasen, Phys. Letters 25B (1967) 554.
[10] R. K. Adair, Phys. Rev. 100 (1955) 1540.
[11] E. de Rafael, Phys. Letters 11 (1964) 260.
[12] A. Kotański, B. Średniawa and K. Zalewski, Nucl. Phys. B23 (1970) 541.
[13] T. D. Lee and C. N. Yang, Phys. Rev. 109 (1958) 1755.